A Review of the Spark Plasma Sintering, Characterization, and Properties of Refractory Nitride-Reinforced Titanium-Based Composites

J. O. Abe[1, 2], O. M. Popoola[2], A. P. I. Popoola[1]

[1]Department of Chemical, Metallurgical and Materials Engineering, Tshwane University of Technology, P.M.B. X680, Pretoria, South Africa.

[2]Centre for Energy and Electric Power, Tshwane University of Technology, Pretoria, South Africa.

ABSTRACT: Titanium alloys are highly favoured in aerospace production for their weight reduction benefits. However, they have several drawbacks, including low hardness, unsatisfactory tribological characteristics, low elastic modulus, and insufficient high-temperature performance (thermal degradation). Certain refractory nitrides, such as aluminium nitride, silicon nitride, titanium nitride, and hexagonal boron nitride, are currently being explored as effective reinforcements to address these limitations, owing to their advantageous properties, including low density, high hardness, exceptional thermal conductivity, and superior wear resistance. This paper reviews the historical context of titanium and its alloys, detailing their classifications and the potential of titanium metal and titanium alloy (Ti6Al4V) matrix composites reinforced with refractory nitrides. It highlights spark plasma sintering (SPS) as a cutting-edge technique for fabricating these composite materials, enabling rapid densification with minimal grain growth. This is a significant improvement compared to traditional sintering methods. The utilization of refractory nitrides as potent reinforcements in various forms, either as individual or combined additives for the synthesis of titanium matrix composites (TMCs) via SPS and characterization of the synthesized TMCs represent a promising research direction with significant implications for aerospace applications and allied industries, aiming to enhance structural, physical, thermal, and mechanical properties.

KEYWORDS: Titanium, Ti6Al4V alloy, Refractory nitrides, Titanium matrix composites, Spark plasma sintering

[Received Feb. 1, 2025; Revised Mar. 6, 2025; Accepted Mar. 16, 2025] Print ISSN: 0189-9546 | Online ISSN: 2437-2110

I. INTRODUCTION

Materials are essential in the aerospace sector throughout the entire aircraft lifecycle, encompassing design, production, certification, flight operations, maintenance, and final disposal after the aircraft's useful life (Jawaid & Thariq, 2018). Aerospace materials encompass the structural components of the airframe that bear the loads encountered during flight operations, as well as the structural elements of the jet engines that sustain the thrust necessary for aircraft propulsion. These materials are crucial for the safety and functionality of aircraft, encompassing key components such as jet engines, turbine blades, and the airframe, which includes the wings, fuselage, empennage, and landing gear (Mouritz, 2012; Donachie, 2020; Leyens & Peters, 2003). For aerospace manufacturers, selecting the optimal materials for engine components or aircraft structures is essential. The utilization of superior materials substantially influences the success or failure of a modern aircraft. The selection of materials for aerospace applications is technically complicated due to exposure to many hostile conditions, including extreme temperatures, ultraviolet radiation, and other atmospheric factors forces (Mouritz, 2012; Leyens & Peters, 2003). The exceptional accomplishments of aircraft manufacturers are closely associated with advancements and innovations in aerospace materials technology. The global pursuit of advanced aviation materials with superior performance attributes continues, as it is crucial for the preservation and enhancement of aerospace technology (Falodun *et al*., 2018; Maseko *et al*., 2018; Mouritz, 2012).

Energy conservation is essential due to the increasing scarcity of resources resulting from their escalating costs, especially in air travel. The fuel consumption of an airplane is a vital parameter for evaluating its operational efficiency. Utilizing materials with a superior strength-to-weight ratio is crucial in aerospace applications to minimize energy consumption. Aerospace engineers consistently strive to save weight while maximizing the strength of each aircraft component (Bhattacharya *et al.*, 2020; Leyens & Peters, 2003). Gas turbine engines are a crucial element of aircraft, enhancing fuel consumption through improved combustion efficiency. Various metals possess distinct weights. Lithium possesses the lowest density of any metal at 0.5 g/cm³, rendering it the lightest, while iridium and osmium are the heaviest metals, with densities of 22.5 g/cm³. Titanium is regarded as the

*Corresponding author: johnabe.fm@gmail.com

doi: http://dx.doi.org/10.63746/njtd.v22i2.3346

heaviest light metal, with a density of 4.51 g/cm³, approximately half that of iron or nickel and twice that of aluminium, the conventional light metal (Bhattacharya *et al.*, 2020; Leyens & Peters, 2003). Initially, during the development of gas turbine engines, heat-resistant nickel-based and steel alloys were the preferred materials. These alloys seem to have become excessively heavy at a certain juncture, requiring their substitution with lighter materials (Dai *et al*., 2016; Mouritz, 2012).

Titanium and its alloys are increasingly becoming significant in research for many uses, particularly in the aerospace and automotive sectors. These alloys are not only lightweight but also exhibit advantageous properties such as high specific strength, low specific gravity, excellent mechanical performance, great chemical resistance, and remarkable biocompatibility. Consequently, they have been designated as the optimal selection for structural, chemical, petrochemical, marine, and biological applications owing to their suitable combination of the aforementioned qualities (Delbari *et al*., 2019; Hayat *et al*., 2019; Adegbenjo, *et al*., 2018; Nsiah-Baafi *et al*., 2022). Compared to other heavyweight classical materials such as nickel-based and steel alloys, titanium and its alloys exhibit a comparatively low modulus of elasticity, insufficient resistance to localized plastic deformation (low hardness), subpar wear resistance, and worse thermal resistance properties. The lightweight and exceptional characteristics of titanium metal or titanium alloy matrix composites (TMCs) enhance these deficiencies (Garbiec *et al*., 2016; Kim *et al*., 2011; Abe *et al*., 2020b). Over the past fifty years, TMCs have emerged as a fast-developing category of industrial materials, supplanting numerous conventional materials in the automotive, aircraft, marine, and sports sectors (Rohatgi *et al*., 2013; Kim *et al*., 2011; Abe *et al*., 2023).

TMCs have been the subject of comprehensive research and development for applications in aerospace airframes and engines (Liu *et al*., 2006; Hayat *et al*., 2019). The principal impetus for their utilization in airframes is their elevated specific modulus, while the engines have gained from their superior specific strength. Titanium aluminide-based TMCs for high-temperature compressor applications, with a temperature capability nearing 760 °C, provide a potential 50% reduction in weight compared to nickel-based superalloys (Singerman & Jackson; 1996; Hayat *et al*., 2019). However, due to the elevated expenses associated with materials and implementation, along with the intricacies of production, the integration of TMCs into high-performance applications has proven challenging. Hayat *et al*. (2019) claimed that there were ongoing efforts in the first phases of TMC research, particularly by the National Aeronautics and Space Administration (NASA), to broaden its application for commercial use. An instance of this was the formation of the Titanium Matrix Composite Turbine Engine Composite Consortium (TMCTECC) program, wherein six American companies worked to develop and integrate titanium matrix composites into large gas turbine engines. The recent advancements and accomplishments of TMCs originated from these prior attempts (Hayat *et al*., 2019; Anderson, 1998).

Refractory nitrides are a distinct type of technologically important ceramics. These materials exhibit an extraordinary amalgamation of distinct properties, including strength (advantageous for structural applications), high hardness and chemical resistance (beneficial for wear and corrosion applications), oxidation resistance and stability at elevated temperatures (essential for high-temperature applications), as well as high thermal conductivity and electrical insulation (valuable for semiconductor applications). As a result, refractory nitrides have been employed in aircraft, automotive, surface technology, high-temperature applications, electrotechnology, electronics, and the fields of chemical and metallurgical engineering. Refractory nitrides encompass the nitrides of elements such as aluminium, silicon, titanium, boron, vanadium, niobium, tantalum, zirconium, and hafnium (Pierson, 1996; Abe *et al*., 2024a). The design of TMCs utilizing refractory nitrides as reinforcing agents, combined with the innovative powder metallurgy technique of spark plasma sintering, which facilitates rapid heating and cooling rates, has been identified as a viable approach for producing superior TMCs with improved properties relative to their unreinforced counterparts (Falodun *et al*., 2018; Abe *et al*., 2023; Abe *et al*., 2024a).

Since the advent of TMCs, research on these materials has proliferated geometrically due to their prospects. A search of the public domain throughout the past five decades, from 1975 to 2025, utilizing the Scopus database, indicates that a total of 2,489 documents have been published about the applications of TMCs, as illustrated in Figure 1 (a). Figures 1 (b) and 1 (c) illustrate additional classifications of the documents by type (in %) and by subject area (in %), respectively. Among this total, there are 1,992 articles, 276 reviews, 151 conference papers, 56 book chapters, 5 books, 2 short surveys, 2 letters, 1 retracted, 1 note, 1 erratum, 1 editorial, and 1 conference review. Nonetheless, it is noteworthy that there are scarce academic reviews accessible on refractory nitride reinforced-TMCs in the public domain.

This paper intends to survey the background information of titanium, titanium alloys, TMCs, refractory nitrides, and spark plasma sintering. The paper also examines specific reviews of literature that underscore significant advancements in TMCs and provides a summary of ongoing initiatives in this evolving field, which includes refractory nitride materials as suitable reinforcements, spark plasma sintering as an effective powder metallurgy processing method, various characterization techniques for the developed TMCs, their ensuing properties advantageous in aerospace applications and related industries.

II. TITANIUM, TITANIUM ALLOYS AND CLASSIFICATIONS

Physicist William Gregor discovered titanium as an element in 1791. Rutile (TiO_2) and ilmenite ($FeTiO_3$) are the two primary varieties of titanium present in raw form as mineral deposits. The Kroll process is the classic titanium ore separation method. Titanium is the fourth most frequent structural metal in the Earth's crust after iron, magnesium, and aluminium. The symbol Ti denotes titanium, a member of the transition metals family. Its elastic modulus is around 115 GPa,

tensile strength ranges between 210 and 1380 MPa, and atomic weight is 47.9 (Gospodinov *et al.,* 2016; Salihu *et al*., 2019).

Titanium can be substantially reinforced through the use of alloying and deformation processing. With a density of approximately 4.50g/cm^3, titanium is a nonmagnetic, low-density element that is approximately 60% the density of steel and superalloys. Titanium possesses excellent heat-transfer capabilities. It has a coefficient of thermal expansion that is marginally lower than that of steel and less than half that of aluminium. The minimum temperature that can be employed for structural purposes is typically 427 °C (800 °F), and the maximum temperature that can be used typically ranges from 538 °C to 595 °C (1000 °F to 1100 °F) depending on the composition (Salihu *et al*., 2019).

It is typically feasible to acquire titanium in both its purified and alloyed forms (Salihu *et al*., 2019). Advancements in refining and production methods have facilitated the significant increase in the use of titanium alloys in recent years, as titanium is rarely used in its pure form (Gospodinov *et al*., 2016). Titanium and its alloys are highly valuable in the chemical and petrochemical, maritime, and biomaterials industries due to their exceptional biocompatibility, outstanding corrosion resistance, and stronger melting points than steels (1668 °C) (Leyens & Peters, 2003; Gospodinov *et al*., 2016). The capacity of various titanium alloys to combine high strength, stiffness, good ductility, low density, and strong corrosion resistance at temperatures ranging from very low to high enables the reduction of weight in aerospace products and other high-performance applications (Adegbenjo *et al*., 2017; Mouritz, 2012).

In pure titanium, the alpha (α) and beta (β) phases are easily distinguishable. The hexagonal close-packed crystalline (HCP) structure of titanium in the α-phase is typically stable from ambient temperature to 882°C (1620°F), as illustrated in Figure 2. On the other hand, the β-phase titanium exhibits a body-centered cubic (BCC) structure that is commonly stable within the temperature range of 882˚C (1620˚F) to 1688˚C (3040˚F). A variety of mechanical and physical properties can be achieved by selectively adding various alloying elements to titanium (Leyens & Peters, 2003; Mouritz, 2012). The following are some of the effects of alloying elements on pure Ti:

- The α-phase is stabilized by the incorporation of aluminium and interstitials (oxygen, nitrogen, and carbon), which raise the transformation temperature of the α-phase to the β-phase. It is widely recognized that this temperature is the β transus temperature.
- The transus temperature is reduced by the majority of alloying additions, including copper, iron, manganese, molybdenum, tantalum, chromium, niobium, and copper, which aid in the stabilization of the β phase.
- Tin and zirconium exhibit neutral solute behavior in titanium, which strengthens the α-phase with negligible influence on the transus temperature (Leyens & Peters, 2003; Mouritz, 2012; Salihu *et al*., 2019).

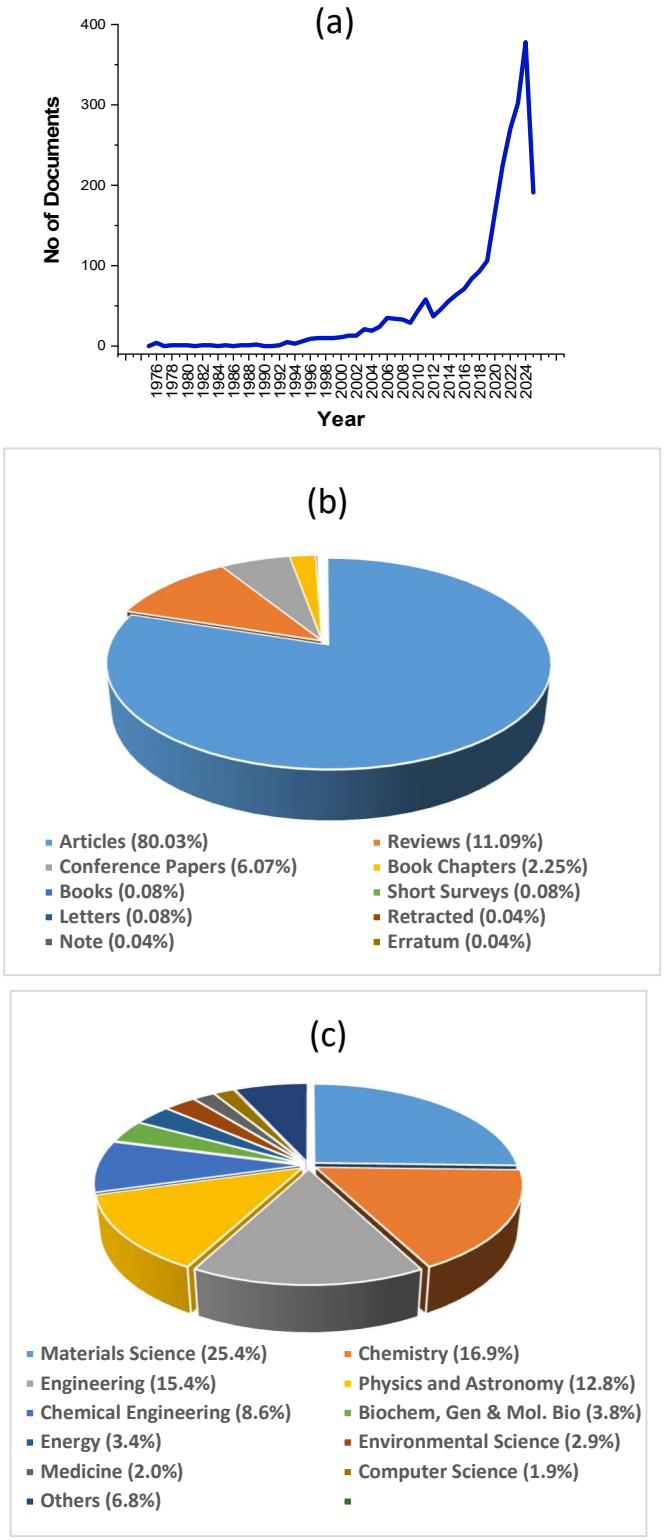

Figure 1: Applications of TMCs: a. Documents by year (in number), b. Documents by type (in %), and c. Documents by subject area (in %)

The microstructures of titanium alloys can be distinguished by different alloy additions and processing. Heat treatment is another way to improve the fatigue strength, toughness, and fracture toughness of these alloys. Titanium

alloys can be classified into five categories according to their composition and room temperature equilibrium behaviour. The included groups are: α-alloys, near-α alloys, α+β alloys, β-alloys, and titanium-based intermetallic compounds, namely those derived from the TiAl compound (Williams & Boyer, 2020; Veiga *et al*., 2012).

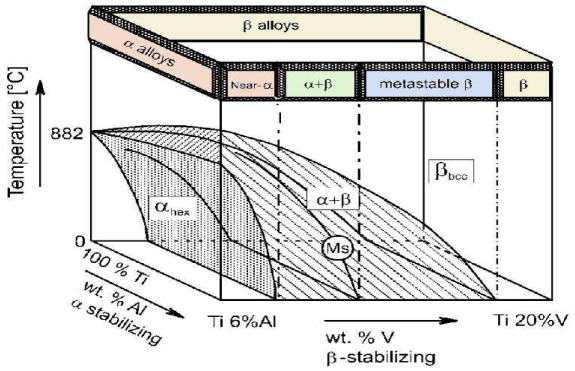

Figure 2: Phase Diagram of Titanium Alloys (Leyens & Peters, 2003)

A. α-alloys

Unalloyed titanium, referred to as commercially pure titanium or CP-Ti, is classified as one of the α-phase alloys. The material predominantly comprises the hexagonal close-packed (HCP) α-phase, with minor quantities (<5 vol.%) of β-phase resulting from the presence of Fe in the source material, sometimes referred to as sponge, either as an intentional inclusion or as a residual contaminant. CP-Ti is offered in four grades (1-4), exhibiting tensile strengths between 240 and 550 MPa. The elevated levels of oxygen, functioning as an interstitial element and a potent solid solution strengthener, are the primary reason for the superior strengths of the higher numbered grades. The primary uses for CP-Ti involve requirements for corrosion resistance and weldability, rather than the elevated strength characteristic of other titanium alloy classes (Donachie, 2020; Veiga *et al*., 2012). Except for specific nickel-base alloys, all titanium alloys exhibit superior corrosion resistance compared to other alloy systems employed in aerospace applications. In aviation, CP-Ti is predominantly employed for hydraulic tubing, various clips and brackets, ducts in the environmental control systems of the passenger cabin, and ducts supplying warm air for the wing leading edge anti-icing systems (Williams & Boyer, 2020).

Similar to CP-Ti, other α-alloys comprise around 95% α-phase; however, they additionally incorporate oxygen, the α-stabilizer aluminium, and the neutral alloying element tin, enhancing their strength compared to CP-Ti. To enhance processing efficiency, this alloy also incorporates minor amounts of α-stabilizing metals such as vanadium. The two most often employed α-phase alloys are Ti-3Al-2.5V (Ti-3-2.5) and Ti-5Al-2.5Sn (Ti-5-2.5), with the latter primarily used at cryogenic temperatures as low as 20K in rocket engine turbomachinery fuel pumps. In addition to the wheel well, which houses the hydraulic lines that operate the main landing gear, Boeing widely utilizes Ti-3-2.5 hydraulic tubing in its aircraft. The hydraulic stainless-steel tubing in the wheel well is utilized because of its superior resistance to foreign object damage (FOD). The Ti-3-2.5 alloy is utilized for the fabrication of brazed or welded honeycomb structures. These alloys can still be formed and joined even if they are stronger than CP grades. Apart from CP-Ti, the α-alloys are more challenging to deal with because they tend to have a high alpha concentration. However, CP-Ti is very workable due to its reduced hardness and flow stresses. They can also be easily welded (Williams & Boyer, 2020; Veiga *et al*., 2012).

B. Near α-alloys

These alloys primarily consist of aluminium, tin, and zirconium, with minor quantities (up to approximately 2 wt. %) of low diffusivity β-stabilizers such as molybdenum and niobium, along with some silicon (up to 0.5 wt. %). Minimal quantities of the residual β-phase are stabilized by the incorporation of molybdenum and niobium at ambient temperature, enhancing strength and facilitating microstructural control throughout processing for improved characteristics and manufacturability. Generally, these alloys cannot undergo heat treatment to alter their strength; nevertheless, they can be utilized at elevated temperatures where creep strength is more significant than tensile qualities. The two predominant near-α alloys are IMI 834 (Ti-5.8Al-4Sn-3.5Zr-0.5Mo-0.7Nb-0.35Si-0.06C), applicable up to around 600°C, and Ti-6Al-2Sn-4Zr-2Mo+Si (Ti-6-2-4-2S), which can be utilized up to a maximum of around 540°C, contingent on loading conditions. IMI834 is presently regarded as the near-α titanium alloy with the highest temperature tolerance available in commercial production. The close alloys exhibit excellent creep resistance and a favourable amalgamation of properties, including tensile ductility, commendable weldability, fatigue resistance, and damage tolerance, despite their inability to undergo heat treatment for enhanced strength. Due to their increased difficulty in rolling and forming compared to α+β and β-alloys, these alloys are infrequently utilized as sheet products. The diminished β-phase content is the reason for this (Donachie, 2020; Leyens & Peters, 2003). In most instances, the maximum service temperature is dictated by the surface absorption of atmospheric oxygen at elevated temperatures rather than by the reduction of strength or creep resistance at those temperatures. This results in the α-phase forming an oxygen-enriched surface layer referred to as the α-case, which is brittle and initiates the onset of fatigue cracks. While these alloys are generally weldable, their processing is more difficult because of reduced formability resulting from the high-volume percentage of solid solution-enhanced α-phase, which contributes to increased strength (Lütjering & Williams, 2007).

C. α+β alloys

A two-phase system, α+β alloys, can be developed by integrating minimal quantities of β-stabilizing alloying elements that preserve the β-phase below the β-transus temperature and extend to ambient temperature. Notably, β-stabilizers can maintain the β-phase at room temperature with minimal amounts. The term "α+β alloys" refers to a category of alloys recognized as high α or near-α alloys, characterized by a significant presence of α-stabilizers and a minimal quantity of β-stabilizers. Adding more β-stabilizers helps to retain an increased proportion of the β-phase at ambient

temperature. Quenching from a high temperature within the α+β region, followed by an aging cycle at a lower temperature, can greatly enhance the strength of such two-phase titanium alloys. The quenching process inhibits the β-phase transformation that would typically occur during gradual cooling. The precipitation of tiny α particles from metastable β during the aging cycle results in a structure that exceeds the strength of the annealed α+β structure (Williams & Boyer, 2020; Veiga *et al*., Davim and Loureiro, 2012).

The Ti6Al4V alloy is undoubtedly the most common titanium alloy in the α+β category. This initial titanium alloy was developed in the early 1950s in the United States at the Illinois Institute of Technology. The α-Ti contributes to the alloy's high strength and fatigue resistance, while the β-Ti influences its superior toughness and creep resistance. The Ti6Al4V alloy is an advanced material known for its high-temperature performance, low density, high specific strength, excellent corrosion resistance, and favourable weldability. Approximately 60% of all titanium alloys produced and used worldwide are made of the Ti6Al4V alloy (Leyens & Peters, 2003; Abe *et al*., 2020a). The success of Ti6Al4V can be attributed to two key factors: firstly, its well-balanced attributes, and secondly, it is the titanium alloy that has undergone the most extensive testing and development, which is particularly advantageous for the aerospace sector that primarily utilizes Ti6Al4V. It constitutes about 80–90% of the titanium used in airframes and around 60% of the titanium used in jet engines (Mouritz, 2012). The applications of the Ti6Al4V alloy are growing across various sectors, including chemical (pressure vessels), marine and offshore industries, architecture, sports and leisure, biomedical (surgical implants and prostheses), mobile and power generation, as well as energy and hydrogen storage devices (Lopez-Suarez *et al*., 2003).

The primary focus in developing other α+β alloys, such as Ti-6-6-2 and IMI 550, was high strength. Ti-6-2-4-6 enables the achievement of high strength coupled with exceptional toughness. Ti-6-2-2-2-2, Ti-55-24-S, and Ti-17 alloys were specifically created for high-temperature applications in gas turbine engines, reaching temperatures around 400 °C. Effectively managing microstructural evolution during high-temperature mechanical processing enhances the mechanical and physical properties of the alloy (Saresh *et al*., Pillai & Mathew, 2007).

D. β alloys

The *β*-alloys represent the most versatile family of titanium alloys. These materials are referred to as β-alloys due to their ability to retain a complete metastable β-phase at room temperature following rapid cooling from the β-phase field. *β*-alloys exhibit the highest strength-to-weight ratio. The alloys integrate strength, toughness, and fatigue resistance in highly advantageous manners at substantial cross sections. These alloys can undergo heat treatment to achieve elevated strengths, are generally more amenable to cold working than *α+β* alloys, and certain variants exhibit superior corrosion resistance compared to commercially pure grades. Compared to *α+β* alloys, certain disadvantages include elevated density, a limited processing window, and greater cost (Williams & Boyer, 2020). Despite their longstanding existence, these materials have just recently attained appeal. Ti-13V-11Cr-3Al was earlier utilized more extensively in the SR-71 Project. At present, the five alloys most commonly employed for structural components are Ti-10-2-3, Beta C, Ti-15-3, TIMETAL 21S, and BT 22, while Ti 17 is utilized for gas turbine engine compressor discs. When properly processed, Ti-10-2-3 exhibits superior strength, toughness, and high cycle fatigue resistance compared to other titanium alloys in its category. Recently produced and presently utilized alloys encompass Beta-CEZ, LCB, and SP 700 (Williams & Boyer, 2020, Donachie, 2020). Besides, metastable β-type titanium alloys demonstrate a low Young's modulus, along with notable mechanical properties and enhanced corrosion resistance. The transformation resulting from deformation, which can modify the Young's modulus, may occur in β-type titanium alloys; therefore, β-type alloys may be advantageous for biomedical applications (Niinomi *et al*., 2016).

E. Titanium-based intermetallic compounds

Besides the near-α alloys, there exists another category of titanium-based alloys with superior temperature resistance. These alloys have been researched for an extended period; but, owing to ductility concerns, their application in actual production engines has only commenced in the past two decades. These alloys are classified as titanium aluminides (TiAl) according to their composition, which is derived from two ordered intermetallic phases: Ti_3Al (α_2) and TiAl (ɤ). The sole alloy currently utilized in production engines is capable of withstanding temperatures above those of conventional titanium alloys and can substitute certain nickel alloys due to its satisfactory high-temperature properties, reaching approximately 725 °C. Moreover, TiAl has a density approximately 50% lower than that of the Ni-based alloys it supplants (Bewlay *et al*., 2016).

The superior thermal strength and enhanced ductility of the α_2 alloys compared to the TiAl-based alloys up to approximately 650°C initially provided them with a competitive advantage. It was revealed that the majority of these initially appealing attributes were obtained from tensile testing conducted in a vacuum or inert gas at standard ASTM E-8 strain rates. Air testing indicated a minor reduction in ductility, however, not to an unacceptable extent. Subsequently, the same alloy was subjected to slow strain rate testing in air, which demonstrated that the reduction in tensile ductility intensified as strain rates decreased, ultimately rendering the alloy brittle. This effect was ascribed to oxygen embrittlement. The research on the α_2 alloys was effectively discontinued due to the severity of the issue (Ward *et al*., 1998; Williams & Boyer, 2020).

III. TITANIUM MATRIX COMPOSITES: TITANIUM METAL AND TITANIUM ALLOY-BASED COMPOSITES

Substantial global progress has been closely tied to the creation and utilization of new materials to address increasing demands and specific requirements in contexts where conventional materials are inadequate. The global demand for high-quality, cost-effective performance materials drives an

in-depth investigation of composite materials. The history of contemporary composites began in the 1930s and has considerably evolved since then. A composite material is formed by amalgamating two or more constituent materials with distinct compositions or dissimilar properties (physical, chemical, mechanical, tribological, thermal, or electrical) to yield an integrated material with superior properties unattainable by the individual components alone. The components of a composite must preserve their distinctiveness inside the finished structure and avoid interacting with each other, especially at high temperatures, since this could lead to premature failure of the composite material. The creation of materials that are stronger, lighter, or more cost-effective than conventional materials is a primary rationale for the utilization of composites, enabling their essential applications across various critical domains. The automobile and aerospace industries have extensively utilized composite materials (Balasubramanian, 2013; Al Islam, & Rahman, 2021).

The essential components of composites consist of a continuous phase referred to as the matrix and one or more discontinuous phases termed reinforcements. The discontinuous phase may exhibit either a firmer or more pliable texture, contingent upon the application. The reinforcement is integrated into the matrix during the composite construction, enhancing the matrix's overall properties. The characteristics of composites are determined by the reinforcement's shape, orientation, distribution, and volume fraction. Composites are classified into three categories according to their matrix material: metal matrix composites (MMCs), ceramic matrix composites (CMCs), and polymer matrix composites (PMCs). Additional classification arises from the type of filler (reinforcement). A composite comprising fibre-based fillers is termed fibrous composite, whereas a composite containing particle-based fillers is referred to as particulate composite (Sharma et al., 2019; Al Islam, & Rahman, 2021).

Metal matrix composites (MMCs) primarily consist of rigid ceramic reinforcements embedded inside a malleable metal or alloy matrix. Metal matrix composites (MMCs) amalgamate the toughness and ductility of metals with the strength and modulus of ceramics (Saheb *et al*., 2012). Due to their enhanced mechanical, thermal, tribological, and thermal conductivity properties compared to conventional materials, they are commonly designated as advanced or superior materials. Aluminium, copper, iron, magnesium, nickel, cobalt, and titanium are the principal matrices utilized in metal matrix composites to date. Most ceramic materials including continuous fibre, chopped fibre, whisker, or particulate serve as reinforcements for metal-matrix composites (MMCs) due to their exceptional strength, stiffness, and low density. Examples of ceramics include silicon carbide, alumina, titanium carbide, titanium nitride, boron carbide, titanium diboride, and graphite (Sharma et al., 2019; Al Islam, & Rahman, 2021). Metal matrix composites provide enhanced specific strength, stiffness, operating temperature, and wear resistance as compared to monolithic metals. It is entirely possible to combine the metal matrix and reinforcing materials effectively to get the required properties for a specific application. Consequently, MMCs possess numerous potential applications across diverse sectors, including automotive, aerospace, electrical, and electronics (Sharma *et al*., 2019; Moghadam *et al*., 2014).

The recent rise in the utilization of titanium and its alloys within the aerospace sector is ascribed to their optimal balance of moderate density and remarkable engineering characteristics, including a high strength-to-weight ratio, stiffness, commendable toughness, low modulus, exceptional corrosion resistance, substantial high-temperature strength, and compatibility with composite structures. Due to these attributes, they are optimal for use in structural, chemical, petrochemical, marine, and biological domains (Guleryuz & Cimenoglu, 2009; Biswas & Majumdar, 2009; Abe *et al*., 2019a). Numerous authors have identified the α/β-Ti6Al4V titanium alloy as fundamental to the aerospace sector due to its superior overall performance compared to other titanium alloy compositions utilized for weight reduction in aerospace applications, especially in airframe and engine components (Boyer, 1996). Nonetheless, owing to several stringent application criteria, such as elevated hardness, wear resistance, and extreme temperature characteristics, the alloy has failed to deliver all requisite features (Abe *et al.,* 2019a; Brice *et al.,* 2016). To maintain the relevance of Ti6Al4V alloy, researchers must diligently address its evident limits. There is a growing demand for the novel development of high-performance materials (Abe *et al*., 2020c; Ramaswamy *et al*., 2016; Callister & Rethwisch, 2015).

In recent decades, considerable research has concentrated on developing composite materials to address the acknowledged limits of titanium and its alloys. A significant advancement thus far is the consolidation of composites utilizing titanium metal and titanium alloys, commonly referred to as titanium matrix composites (TMCs). Numerous advantages of TMCs development have been recorded in prior studies (Ramaswamy *et al*., 2016; Xiang *et al*., 2012; Abe *et al*., 2020a). TMCs provide enhanced specific strength, specific stiffness, wear resistance, hardness, thermal stability, and high-temperature durability compared to titanium alloys. They also manufacture a composite material with properties that differ from those of the individual constituents. The aerospace sector has led the advancement of TMCs for almost fifty years (Kim *et al*., 2011). Numerous prior research (Falodun *et al*., 2023; Wei *et al*., 2012; Garbiec *et al*., 2019; Nsiah-Baafi *et al*., 2022; Balaji & Kumaran, 2015; Okoro *et al*., 2019; Bai *et al*., 2019; Lagos *et al*., 2016; Cao *et al*., 2015; Ayodele *et al*., 2023) have recorded substantial advancements in TMCs fortified with ceramic materials. Overcoming the substantial manufacturing costs of TMCs remains essential for a successful shift to economical commercial production (Boyer, 1996; Kim *et al*., 2011).

Titanium matrix composites are often categorized into two types: continuously reinforced TMCs and discontinuously reinforced TMCs, based on the reinforcement methods utilized (Callister & Rethwisch, 2015; Hayat *et al*., 2019).

A. Continuously Reinforced Titanium Matrix Composites (CRTMCs)

Titanium matrix composites that are continuously reinforced (CRTMCs) can be produced by using a variety of filaments or fibres for reinforcement. The directional reliance

of this form of reinforcement poses a vulnerability due to its vertical orientation, complex designs, and additional coating cost issue.

CRTMCs can be fabricated using various filaments or fibres for reinforcement. The directional dependence of this reinforcement type presents a weakness owing to its vertical alignment, intricate designs, and the expense associated with additional coatings (Abe *et al*., 2020a; Kim *et al*., 2011; Kgoete *et al*., 2019).

B. Discontinuously Reinforced Titanium Matrix Composites (DRTMCs)

Discontinuously reinforced titanium matrix composites (DRTMCs) incorporate reinforcements such as chopped fibres, whiskers, or particles, unlike continuously reinforced DRTMCs. Despite having relatively poor mechanical properties, DRTMCs are highly favoured for their affordability, excellent repeatability, straightforward production, and enhanced isotropic characteristics, facilitating a diverse array of reinforcement kinds (Abe *et al*., 2020a; Kim *et al*., 2011; Kgoete *et al*., 2019). Table 1 provides a summary of notable advancements in DRTMCs derived from prior research.

IV. REFRACTORY NITRIDE REINFORCEMENTS

Nitrogen predominantly forms compounds when it interacts with other elements. Nitrides are exclusively compounds formed when nitrogen reacts with elements that possess lower or almost equivalent electronegativity. Figure 3 illustrates that nitrides can be categorized into five distinct categories according to their electronic structure and bonding characteristics: interstitial nitrides, covalent nitrides, intermediate nitrides, salt-like nitrides, and volatile (molecule-forming) nitrides. Only a subset of the interstitial and covalent nitrides within these categories, specifically the covalent nitrides of boron, aluminium, and silicon, along with the nitrides of the nine transition metals from Groups IV, V, and VI, as well as those from the fourth, fifth, and sixth periods, satisfy the criteria for being classified as refractory. Nonetheless, most salt-like and intermediate nitrides lack chemical stability despite possessing high melting points, and hence, they are not classified as refractory nitrides (Pierson, 1996; Riedel, 2000).

Refractory nitrides are materials specifically chosen for their elevated melting points (often over 1800 °C) and significant chemical stability. Figure 3 illustrates the refractory nitrides, represented in bold typeface; interstitial nitrides are located in BOX A, covalent nitrides in BOX B, intermediate nitrides in BOX C, salt-like nitrides in BOX D, and volatile (molecule-forming) nitrides in BOX E. Refractory nitrides include the nitrides of elements such as Ti, V, Ta, Nb, Zr, B, Hf, Al, and Si. They constitute a group of technologically significant nitrides, akin to ceramics, characterized by an exceptional amalgamation of properties, including notable attributes such as strength (for structural applications), elevated hardness and chemical resistance (for wear and corrosion applications), a high melting point (>1800 °C), thermal stability at elevated temperatures, and oxidation resistance (for high-temperature applications); similar to metals, they exhibit high thermal conductivity and electrical insulation (for semiconductor applications). Consequently, they have achieved extensive use in the aerospace, automotive, surface, high-temperature technology, electrotechnology, electronics, chemical, and metallurgical engineering sectors (Pierson, 1996; Riedel, 2000; Abe *et al*., 2024b; Jiang *et al*., 2015).

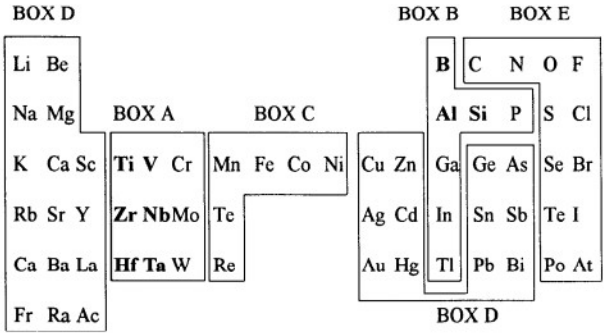

Figure 3: Classification of the Nitrides-Forming Elements (Pierson, 1996)

Furthermore, literature has recorded the effective development and exceptional characteristics of TMCs reinforced with refractory nitrides. The prevalent refractory nitrides documented are the nitrides of aluminium (Abe *et al*., 2020a; Abe *et al*., 2020b; Abe *et al*., 2020c; Abe *et al*., 2022), silicon (Kgoete *et al*., 2019), titanium (Falodun *et al*., 2019; Abe *et al*., 2020a; Abe *et al*., 2020b; Kgoete *et al*., 2019; Abe *et al*., 2023), and hexagonal boron nitride (Abe *et al*., 2020a; Abe *et al*., 2020b; Abe *et al*., 2020c; Abe *et al*., 2022; Abe *et al*., 2023). Consequently, these nitrides have undergone widespread research owing to their advantageous features, which encompass elevated hardness, high melting point, substantial thermal conductivity, commendable high-temperature stability, significant chemical stability, and exceptional wear resistance (Abe *et al*., 2019b; Abe *et al*., 2020b; Kgoete *et al*., 2019; Falodun *et al*., 2017; Abe *et al*., 2023).

A. Aluminium Nitride

Aluminium nitride is also known as solid aluminium nitride (AlN). Although it was initially synthesized in 1862, it was not until the middle of the 1980s that the possibility of its use in microelectronics prompted the production of high-quality, economically feasible material. AlN can be produced either by carbothermal reduction of aluminium oxide (alumina) or aluminium can be directly nitrided in the presence of gaseous nitrogen or ammonia in a reaction that takes place at very high temperatures (>1800 °C). Without the aid of liquid forming chemicals, the material is covalently linked and resists sintering. To produce a dense technical-grade material, sintering aids like Y_2O_3 or CaO must be used in conjunction with hot pressing (Cheng, *et al*., 2020; Chasnyk *et al*., 2020; Ras *et al*., 2014).

The primary thermodynamically stable crystal structure of AlN is wurtzite as shown in Figure 4; however, it also possesses a metastable cubic zincblende phase that is generally manufactured in thin film form. At elevated pressures,

superconductivity in the AlN cubic phase (zb-AlN) is expected (Cheng *et al*., 2020; Chasnyk *et al*., 2020). Al and N alternate along the c-axis in the AlN wurtzite crystal structure. Each link has four atoms per unit cell and is tetrahedrally coordinated (Dancy *et al*., 2015). The spontaneous polarization of wurtzite AlN is one of its special inherent features. The strong ionic nature of chemical bonding in wurtzite AlN, which results from the stark contrast in electronegativity between the nitrogen and aluminium atoms, is the cause of spontaneous polarization. At ambient temperature, the band gap of its wurtzite phase (w-AlN) is around 6 eV (Cheng, *et al*., 2020; Chasnyk *et al*., 2020). The schematic diagram of AlN crystal structure is shown in Figure 4.

In inert atmospheres, decomposition of AlN takes place at about 1,800 °C (2,070 K; 3,270 °F) in a vacuum. Above 700 °C (973 K; 1,292 °F), surface oxidation takes place in the atmosphere. Surface oxide layers as thin as 5–10 nm have been found at ambient temperature. The material is protected up to 1,370 °C (1,640 K; 2,500 °F) by this oxide layer. Bulk oxidation takes place above this temperature. Up to 980 °C (1,250 K; 1,800 °F), AlN remains stable in hydrogen and carbon dioxide atmospheres (Berger, 2020). Grain-boundary attack causes the material to dissolve slowly in mineral acids, while grain-attack on AlN grains causes it to dissolve slowly in strong alkalis. In water, the substance hydrolyses slowly. Most molten salts, such as cryolite and chlorides, cannot harm AlN (Pradhan *et al*., 2015).

Aluminium nitride is an electrical insulator, dissociates at 2500 °C at atmospheric pressure, has a low density, and as a single crystal has a high inherent thermal conductivity (see Table 2) while not melting (Berger, 2020; Cheng *et al*., 2020; Morkoç, 2001). More details on the properties of AlN are given in Table 2. Optoelectronics, optical storage media dielectric layers, electronic substrates, chip carriers (where high heat conductivity is crucial), steel production, and semiconductor manufacturing are a few industries where AlN is used. Another area of widespread application of AlN is in aerospace and defence sectors because of its exceptional thermal stability and resilience to a wide range of extreme conditions. Numerous investigations on the various uses of AlN as reinforcing materials for metal-matrix composites (MMCs) have been carried out, and the resulting composites have demonstrated improved mechanical, tribological, corrosion-resistant, and high-temperature properties (Liu *et al*., 2019; Kaliappan *et al*., 2022; Khrustalyov *et al*., 2017; Wang *et al*., 2022; Singh *et al*., 2023; Falcon-Franco *et al*., 2016; Fale *et al*., 2015; Ma *et al*., 2016; Kumar & Venkatesh, 2019; Radhika & Raghu, 2017; Chen *et al*., 2023).

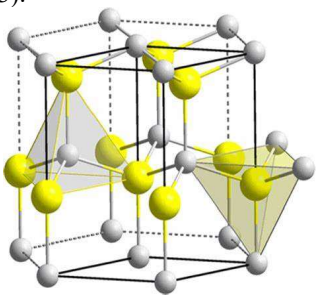

Figure 4: Schematic Diagram of AlN Crystal Structure (Singh *et al*., 2021b)

B. Silicon Nitride

Silicon nitride (Si_3N_4) is chemically developed by the combination of silicon and nitrogen. It is the most thermodynamically stable and important silicon nitride from a commercial perspective. It was manufactured in an effort to develop materials that were completely dense and extremely durable in the 1960s and 1970s. One of the main forces behind the development of advanced reciprocating and turbine engines was the substitution of ceramics for metals in order to attain better operating temperatures and efficiency. Producing completely dense pure silicon nitride is difficult. It is not a common practice to heat this covalently bound material above 1850ºC because it will split into silicon and nitrogen. It does not sinter readily either. Dense silicon nitride can only be produced using indirect bonding procedures, such as small chemical inputs to aid in densification. These materials, sometimes known as sintering aids, often result in some degree of liquid phase sintering (Morkoç, 2001; Van Tran & Duc La, 2018).

The three crystallographic structures seen in silicon nitride are known as α, β, and γ phases. The two most common phases of Si_3N_4 that can be formed at normal pressure are α and β phases. The γ phase can only be synthesized at high temperatures and pressures. The structure of α-Si_3N_4 with a stacking sequence is generally harder than that of β-Si_3N_4, but the β-phase is believed to be more stable at high temperatures (Hampshire, 2007; Riley, 2020; Fayomi *et al*., 2020). Figure 5 shows the schematic diagram of the structures of α-Si_3N_4 and β-Si_3N_4, where silicon atoms (in black colour) and nitrogen (in green colour) form hexagonal crystal structures (Hampshire, 2007; Riley, 2020; Fayomi *et al*., 2020).

Silicon nitride is a dark grey, extremely combustible substance that has a low specific heat. It is fairly hard, very strong and exhibits excellent heat stability. The exceptional properties of silicon nitride, including its high temperature and thermal shock resistance, low density, high corrosion resistance, and other mechanical properties, have made it one of the most essential engineering ceramics for any practical applications. Some characteristics of Si_3N_4 are highlighted in Table 2 (Lad, 1996; Dow *et al*., 2017; Heimann, 2023). Silicon nitride is currently employed in aerospace and automobile fields and in niche market applications such as turbochargers, bearings, reciprocating engine components, metal cutting and shaping tools, and hot metal handling (Hampshire, 2007; Fayomi *et al*., 2020; Van Tran & Duc La, 2018). Many investigations have been carried out lately on the various uses of Si_3N_4 as reinforcing materials for metal-matrix composites (MMCs), exhibiting enhancements in the resulting mechanical, tribological, corrosion, and high-temperature characteristics of the produced composites (Mattli *et al*., 2019; Parveen *et al*., 2019; Maddaiah & Veeresh, 2023; Manghnani *et al*., 2021; Kumar *et al*., 2019; Raja *et al*., 2022; Mahato & Mondal, 2021; Reddy, 2003; Hanumantharayappa *et al*., 2021; López-López *et al*., 2023; Kumar *et al*., 2022; Song *et al*., 2022; Ajay *et al*., 2023; Tanwir *et al*., 2023; Dhinakarraj *et al*., 2023).

Table 1: Overview of recent documented advancements in DRTMCs

Matrix Material	**Reinforcement (vol. %)**	**Processing Technique**	**Some Selected Physical and Mechanical Properties**				**References**
			Relative Density (gcm^{-3})	Hardness	Tensile Strength (MPa)	Ductility (%)	
Ti	5% TiB	VAR+HS	-	-	787	12.5	Tsang *et al.* (1997)
Ti	15% TiB	VAR+HS	-	-	903	0.4	Tsang *et al*. (1997)
Ti	20% TiB	PM	-	-	673	0	Chandran & Panda (2002)
Ti	4% TiB+0.97% TiC	PM	-	-	876	14.2	Kondon *et al*. (2015)
Ti	6.49%TiB+1.61% TiC	PM	-	-	995	7.8	Kondon *et al*. (2015)
Ti	10.93%TiB+2.81% TiC	PM	-	-	1138	2.6	Kondon *et al*. (2015)
Ti	5 %TiB+1.17% Y_2O_3	AM	-	52.5HRC	-	-	Geng *et al*. (2004)
Ti	5 %TiB+3.49% Y_2O_3	AM	-	48.2HRC	-	-	Geng *et al*. (2004)
Ti	5 %TiB+5.79% Y_2O_3	AM	-	45.5HRC	-	-	Geng *et al*. (2004)
Ti	5 %TiB+8.64% Y_2O_3	AM	-	38.0HRC	-	-	Geng *et al*. (2004)
Ti	0.94 wt. % B_4C	VIM	-	239HRB	-	-	Kim *et al*. (2011)
Ti	1.88 wt. % B_4C	VIM	-	259HRB	-	-	Kim *et al*. (2011)
Ti	3.76 wt. % B_4C	VIM	-	306HRB	-	-	Kim *et al*. (2011)
Ti	0.2 wt. % MWCNTs	SPS	99.69%	2GPa	898	-	Wang *et al*. (2015)
Ti	0.4 wt. % MWCNTs	SPS	99.44%	2.18GPa	1092	-	Wang *et al*. (2015)
Ti	0.6 wt. % MWCNTs	SPS	99.31%	2.3GPa	1052	-	Wang *et al*. (2015)
Ti	0.8 wt. % MWCNTs	SPS	99.13%	2.39GPa	1015	-	Wang *et al*. (2015)
Ti	1.0 wt. % MWCNTs	SPS	99.01%	2.4GPa	853	-	Wang *et al*. (2015)
Ti	2 wt. % GnP	SPS	~100	615HV	-	-	Vasanthakumar *et al.* (2019)
Ti	2 wt. % g-C_3N_4	SPS	~100	827HV	-	-	Vasanthakumar *et al.* (2019)
Ti6Al4V	20% TiB	PM+E	-	-	1215	0.5	Gorsse & Miracle (2003)
Ti6Al4V	40% TiB	MA+HP	-	-	1018	0.1	Gorsse & Miracle (2003)
Ti6Al4V	40% TiB	PM+E	-	-	864	0	Gorsse & Miracle (2003)
Ti6Al4V	5% SiCp	PM	-	460HV	-	-	Sivakumar *et al*. (2017)
Ti6Al4V	10% SiCp	PM	-	369HV	-	-	Sivakumar *et al*. (2017)
Ti6Al4V	15% SiCp	PM	-	315HV	-	-	Sivakumar *et al*. (2017)
Ti6Al4V	5% TiC	SPS	99.70%	-	995	3	Lagos *et al*. (2016)
Ti6Al4V	10% TiC	SPS	99.60%	-	1060	3	Lagos *et al*. (2016)
Ti6Al4V	3 wt. % Si_3N_4+15 wt. % ZrO_2	SPS	99.94	865.7MPa	-	-	Ogunmefun *et al.* (2024)
Ti6Al4V	3 wt. % Si_3N_4+10 wt.% ZrO_2	SPS	97.73	670.11MPa	-	-	Ogunmefun *et al.* (2024)
Ti6Al4V	3 wt. % Si_3N_4+5 wt. % ZrO_2	SPS	97.11	657.27MPa	-	-	Ogunmefun *et al.* (2024)
Ti6Al4V	0.5 wt. % GO	SPS	99.1	-	1040.1	5.3	Song *et al.* (2021)
Ti6Al4V	1.0 wt. % GO	SPS	99.0	-	1053.4	1.8	Song *et al.* (2021)
Ti6Al4V	3 wt. % TiC	SPS	-	465 HV	-	-	Singh *et al.* (2021a)
Ti6Al4V	3 wt. % TiC+0.05wt.% B	SPS	-	479 HV	-	-	Singh *et al.* (2021a)
Ti6Al4V	3 wt. % TiC+0.1wt.% B	SPS	-	489 HV	-	-	Singh *et al.* (2021a)
Ti6Al4V	0.1 GR	SPS	-	-	895	21.8	Zhang *et al.* (2021)
Ti6Al4V	0.4 GR	SPS	-	-	906	15.3	Zhang *et al.* (2021)
Ti6Al4V	0.05 nano-TiC/0.1 GR	SPS	-	-	868	22.6	Zhang *et al.* (2021)
Ti6Al4V	0.05 nano-TiC/0.4 GR	SPS	-	-	1033	13.2	Zhang *et al.* (2021)

Ti6Al4V	0.25 nano-TiC/0.2 GR	SPS	-	-	950	15.6	Zhang *et al.* (2021)
Ti6Al4V	0.05 nano-TiC/0.3 GR	SPS	-	-	976	14.8	Zhang *et al.* (2021)
Ti6Al4V	0.4 nano-TiC/0.05 GR	SPS	-	-	904	19.1	Zhang *et al.* (2021)
Ti24.3Mo	34% TiB	PM+HP+HT		-	1105	0.9	Panda & Ravi (2003)
Ti53Nb	34% TiB	PM+HP+HT		-	724	1.7	Panda & Ravi (2003)
Ti6.4Fe10.3Mo	34% TiB	PM+HP	-	-	736	0.5	Panda & Ravi (2003)
Ti4Fe7.3Mo	10% TiB	MA+SPS	99.60%	-	-	-	Feng *et al*. (2004)
Ti22Al27Nb	6.5% TiB	IM	-	-	992	4	Emura *et al*. (2004)
Ti22Al27Nb	6.5% TiB	GA+PM	-	-	1260	2.3	Emura *et al*. (2004)
Ti6Al2Zr1Mo1V	5% TiC	LMD	-	-	925.87	4.32	Liu *et al*. (2009)
Ti6Al2Zr1Mo1V	10% TiC	LMD	-	-	845.27	1.23	Liu *et al*. (2009)
Ti6Al2Zr1Mo1V	15% TiC	LMD	-	-	806.38	1.33	Liu *et al*. (2009)
Ti4.5Al6.8Mo1.5Fe	5% TiB	HVC	97.90%	335HV	1038	2.19	Yan *et al*. (2014)
Ti4.5Al6.8Mo1.5Fe	10% TiB	HVC	98.20%	392HV	1147	-	Yan *et al*. (2014)
Ti4.5Al6.8Mo1.5Fe	15% TiB	HVC	98.30%	428HV	741	-	Yan *et al*. (2014)
Ti6Al7Nb	0.5 wt. % TiB_2	SPS	>99.5	381.76HV	-	-	Singh *et al*. (2022a)
Ti6Al7Nb	1.5 wt. % TiB_2	SPS	>99.5	438.88HV	-	-	Singh *et al*. (2022a)
Ti6Al7Nb	3.0 wt. % TiB_2	SPS	>99.5	495.96HV	-	-	Singh *et al*. (2022a)

Note: *VAR = Vacuum Arc Remelting; HS = Hot Swaged; PM = Powder Metallurgy; AM = Arc Melting; VIM = Vacuum Induction Melting; SPS = Spark Plasma Sintering; HE = Hot Extrusion; MA = Mechanical Alloying; HP = Hot Pressing; HT= Heat Treatment; IM = Ingot Metallurgy; GA = Gas Atomization; LMD = Laser Melted Deposition; HVC = High Velocity Compaction*

Table 2: Overview of some selected information on the studied refractory nitrides

Name of refractory nitride	**Chemical formula**	**Appearance or colour**	**Crystal structure**	**Density ($g \cdot cm^{-3}$)**	**Molar mass ($g \cdot mol^{-1}$)**	**Hardness**	**Melting point (°C)**	**Thermal conductivity (W/m.K)**	**References**
Aluminium nitride	AlN	Translucent grey	Wurtzite	3.15-3.21	40.99	1200 $kgmm^2$ (Knoop)	2,200 °C	~140-320	Berger (2020); Cheng *et al.* (2020); Morkoc (2001)
Silicon nitride	Si_3N_4	Dark grey	Hexagonal	3.17	140.283	1580 $kgmm^2$ (Knoop)	1,900 °C	~16-19	Lad (1996); Dow *et al*. (2017); Heimann (2023)
Titanium nitride	TiN	Brown as a pure solid; coating of golden colour	Face-centred-cubic (FCC)	5.21	61.874	1.8-2.1 GPa (Vickers)	2,947 °C	29	Stone *et al*. (1991); Pierson (1996); Zhang *et al.* (2012)
Hexagonal boron nitride	*h*-BN	White	Hexagonal	2.1	24.82	1.3-1.5 GPa (Vickers)	2,973 °C	600	Ciftci (2013); Zheng *et al*. (2018)

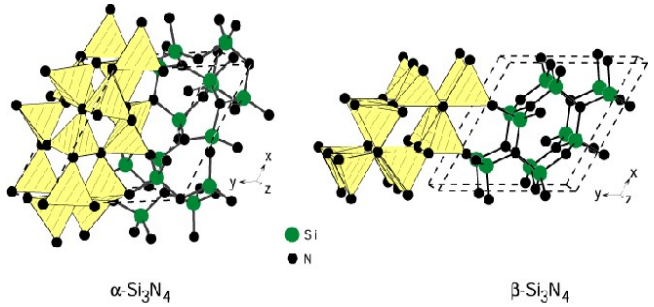

Figure 5: Schematic Diagrams of α-Si_3N_4 and β-Si_3N_4 Crystal Structures (Van Tran & Duc La, 2018)

C. Titanium Nitride

Titanium nitride (TiN) is alternatively referred to as Tinite. The standard formation of TiN has a NaCl-type crystal structure with a stoichiometry of approximately 1:1. It is part of a face-centred cubic (FCC) lattice. The FCC structure has nitrogen atoms at its vertices, with the titanium atom situated at the (1/2, 0, 0) coordinate within the FCC lattice. Due to thenon-stoichiometric nature of the nitride, its thermodynamically stable compounds (TiNx) exhibit x values ranging from 0.6 to 1.2. This suggests that the nitrogen content may vary within a specific range without impacting the TiN structure (Lad, 1996; Toth, 1971; Saurabh *et al*., 2022). Figure 6 illustrates the schematic representation of the titanium nitride structure.

Under standard atmospheric conditions, TiN commences oxidation at around 800 °C. Laboratory experiments indicate that it remains chemically stable at 20 °C; nevertheless, elevated temperatures may lead to slow degradation by concentrated acid solutions (Riedel, 2000). At cryogenic temperatures, titanium nitride (TiN) demonstrates superconductivity, with single crystals achieving a critical temperature of up to 6.0 K (Spengler, 1978). Extensive study has been conducted on superconductivity in thin-film TiN. The superconducting properties significantly fluctuate depending on sample preparation and may be entirely inhibited at a superconductor-insulator transition. Upon cooling to near absolute zero, a thin layer of TiN was converted into the first scientifically recognized superinsulator, exhibiting a dramatic increase in resistance by 100,000 (Saurabh *et al*., 2022; Baturina, 2007; Milošev *et al*., 1997).

Titanium nitride is brown in appearance, but when coated, it looks gold. It is an electrical conductor. The coefficient of friction for TiN on another TiN surface (non-lubricated) will range from 0.4 to 0.9, contingent upon the substrate material and surface polish. Additional features of TiN are presented in Table 2 (Pierson, 1996; Stone *et al*., 1991; Zhang *et al*., 2012). Titanium nitride is a highly durable ceramic substance extensively utilized to enhance the surface properties of components composed of titanium, aluminium, and iron alloys. Titanium nitride is utilized as a thin coating to enhance and safeguard cutting and sliding surfaces, for the outside of medical implants owing to its non-toxic properties, and for aesthetic purposes due to its golden hue. Recent studies have documented the superior mechanical, tribological, corrosion, and high-temperature characteristics of metal matrix composites reinforced with TiN (Kganakga *et al*., 2020; Maja *et al*., 2018; Franczak & Karwan-Baczewska, 2017; Reddy, 2013; Krishna *et al*., 2022; Li *et al*., 2019; Mahesh *et al*., 2020; Gao *et al*., 2020; Akinwamide *et al*., 2020; Chen & Ou, 2020; Alavala, 2016; Akinwamide *et al*., 2019).

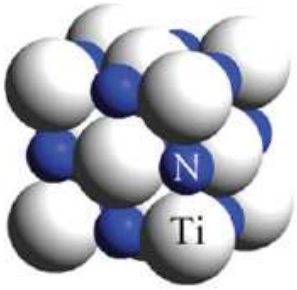

Figure 6: Schematic Diagram of Bulk TiN Crystal Structure (Zhang *et al*., 2012)

D. Hexagonal Boron Nitride

The hexagonal structure of boron nitride (BN) is commonly referred to as hexagonal boron nitride (*h*-BN). The nitride exhibits structural similarity to the lubricious, smooth, platy hexagonal configuration of carbon graphite, so it is frequently termed "white graphite". Figure 7 illustrates that hexagonal boron nitride consists of layers of covalently bound boron (solid spheres) and nitrogen (open spheres) atoms organized in a sp2 planar configuration, creating a two-dimensional network. The boron (nitrogen) atoms possess an unoccupied (occupied) pz orbital oriented perpendicular to the planar B-N layer, and their covalent radius is approximately 20% larger than that of nitrogen (Lad, 1996; Ciftci, 2013; Zheng *et al*., 2018). Although discovered in the early 1800s, the commercial development of the substance did not transpire until the later half of the 1900s. Hexagonal boron nitride powder can be synthesized via ammonolysis or nitridation of boric oxide at elevated temperatures. Under standard conditions, the nitride is considered the most stable phase of boron nitride (Kim *et al*., 2012; Duan *et al*., 2016).

Hexagonal boron nitride is a highly versatile ceramic material employed across various domains due to its unique amalgamation of attributes, including low density, superior lubrication characteristics (minimal coefficient of friction), high-temperature stability, chemical inertness, thermal shock resistance, ease of workability, exceptional thermal conductivity, non-toxicity, and environmental safety (Lad, 1996; Lipp, Schwetz & Hunold, 1989; Eichler & Christoph, 2008). Table 2 presents more details on the properties of *h*-BN (Ciftci, 2013; Zheng, Cox and Li; 2018). It can be employed as coatings, powders, or sintered forms composed of either pure h-BN or composites. Applications of *h*-BN and *h*-BN-containing composites are present in metallurgy, chemistry, high-temperature technology, electronics, and aerospace engineering (Klöpfer, 2006; Ertuğ, 2013; Abe *et al*., 2019b). Recent studies have demonstrated that *h*-BN serves as an effective reinforcement for MMCs, exhibiting superior mechanical, chemical, lubricating, and high-temperature properties (Karabacak *et al*., 2023; Singh *et al*., 2022b; Zhu *et al*., 2019; Khalaj *et al*., 2020; Aydin & Turan 2020; Paulraj & Harichandran, 2020; Hussain *et al*., 2022; Chand &

Chandrasekhar, 2020; Reddy *et al*., 2018; Firestein *et al*., 2017).

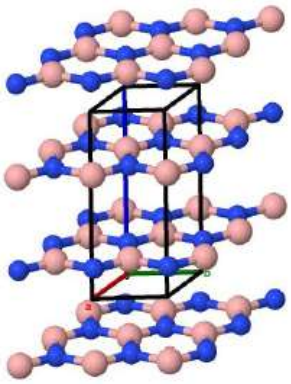

Figure 7: Schematic Diagram of *h*-BN Crystal Structure (Ciftci, 2013)

V. POWDER METALLURGY OF TITANIUM MATRIX COMPOSITES

Processability is the primary factor that dictates the required technology and cost of a composite material. This describes the process by which the constituent materials are combined to produce the composite. Thus, the cohesiveness of a composite's constituent elements affects its processability. The processing often occurs at elevated pressures and/or temperatures for a specified duration, contingent upon the condition of the matrix material. Due to the disparate thermal shrinkage rates of the matrix and reinforcement, it is essential to exercise caution to avert the weakening or debonding of the matrix-reinforcement interface that may occur at elevated temperatures or during subsequent cooling. If this occurs, it diminishes the efficacy of the reinforcement, hence reducing the mechanical properties of the composite. This issue typically exacerbates in MMCs due to the comparatively elevated processing temperatures required (Sharma *et al*., 2019; Hayat *et al*., 2019).

There are numerous ways to produce TMCs. The selection of an appropriate processing path is primarily driven by the intended use, matrix materials, reinforcement materials, and their type, quantity, and distribution. Even with the same composition and quantities of the constituent materials, different profiles can be obtained by altering the shape of the reinforcement materials and the production method (processing and finishing) (Hayat et al., 2019). Producing titanium matrix composites (TMCs) reinforced with ex-situ additive particles using conventional ingot metallurgical processes is highly tough due to the strong chemical reactivity of titanium. The powder metallurgy (PM) method is extensively employed to manufacture TMC products. Generally, PM procedures are regarded as very efficient and appropriate manufacturing techniques for DRTCs. The critical parameters for ensuring the proper processing of DRTCs by PM are the uniform mixing and dispersion of powder particles. The use of a surface coating can enhance homogeneous dispersion. The selection of reinforcements, including their dimensions, morphology, material composition, and the adhesion between the matrix and the reinforcements, significantly influences the final properties of the composites. The incorporation of reinforcements into the matrix can be accomplished via ex-situ or in-situ processing, contingent upon the interactions that transpire between the reinforcements and the matrix (Hayat *et al*., 2019; Kondoh, 2015; Huang & Geng, 2017).

A. Powder Metallurgy Processing Methods

1) Ex-situ PM processing method

Ex-situ processing techniques are employed in titanium powder metallurgy utilizing thermodynamically stable additives such as silicon carbide, titanium carbide, titanium diboride, and zirconium carbide. No entirely new compounds are generated during the sintering and consolidation operations. The size and shape of the additive particles remain the same before and after sintering, unless further mechanical deformation is performed on purpose. In addition to providing better mechanical properties, ex-situ manufacturing of DRTCs improves wear resistance under dry sliding conditions by increasing friction coefficient stability (Kondoh, 2015; Hayat *et al*., 2019). The primary limitation that has prevented the widespread application of ex-situ techniques to produce DRTCs is inadequate matrix-reinforcement interfacial bonding. Conversely, DRTCs produced using in-situ synthesis methods are attractive because of their enhanced properties, isotropic features, and inexpensive cost (Jeje *et al*., 2021a; Hayat *et al*., 2019).

2) In-situ PM processing method

In-situ processing involves the amalgamation of elements like boron, carbon, and nitrogen with a highly reactive titanium matrix to generate stable particles or needle-like reinforcements through solid-state reactions. Common precursors utilized in in-situ processing comprise silicon nitride, boron carbide, titanium diboride, and chromium carbide. The utilization of titanium powder may result in an interaction with TiB_2 particles during sintering, leading to the formation of TiB whiskers that are subsequently dispersed throughout the matrix as reinforcement (Jeje *et al*., 2021a; Hayat *et al*., 2019). Enhanced tribological performance is attained through the establishment of robust bonding between matrix and reinforcements during in-situ processing. Furthermore, in-situ techniques produce composites exhibiting superior creep and oxidation resistance, alongside elevated specific strength and modulus. Nevertheless, heightened vigilance is necessary to guarantee that the in-situ reactions are meticulously regulated to avert the formation of interfacial defects (Kondoh, 2015; Jeje *et al*., 2021a; Hayat *et al*., 2019).

Other methods that have been used to produce in-situ DRTCs besides traditional powder metallurgy include additive manufacturing, ingot metallurgy, and self-propagation high-temperature synthesis (SHS) (Jeje *et al*., 2021a; Hayat *et al*., 2019). These other methods are not included in the scope of the current review and, therefore, are not covered beyond this.

B. Spark Plasma Sintering

Spark plasma sintering (SPS) is an advanced powder metallurgy manufacturing technique, also known as pulsed electric current sintering (PECS) and field-assisted sintering methods (FAST). It is among the most recent, sophisticated,

and novel non-conventional sintering processes accessible. The substantial advantages of SPS compared to traditional sintering methods have attracted the attention of many academics and engineers worldwide. The SPS approach is particularly unique among powder metallurgy methods due to its heating mechanism (Garbiec *et al*., 2016; Ayodele *et al*., 2021; Ayodele *et al*., 2023; Jeje *et al*., 2021a). It employs both internal and external heating sources, chiefly via an electric spark discharge termed spark plasma, generated utilizing low-voltage, high-pulse direct current (Joule heating) in conjunction with uniaxial pressure, facilitating rapid heating and cooling rates. This differs from traditional sintering, in which heat is produced by an external source and conveyed to the component through conduction, convection, and radiation (Matizamhuka, 2016; Kessel *et al*., 2009; Al-Aqeeli, 2013; Diouf & Molinari, 2012; Cavaliere *et al*., 2019).

The basic configuration of an SPS machine, a simple depiction of the SPS process and its mechanism are shown in Figures 8, 9, and 10, respectively. During SPS operation, the powder components are quantified and meticulously measured in a container, and the powder mixture is homogenized for a specified duration at an optimal operating speed in a tubular mixer. An automated SPS machine is utilized to consolidate the mixed particles in a vacuum environment. The upper and lower punches conveyed applied pressure and pulsed direct current to the powders, integrating the consolidation and compaction processes into a singular unit operation (see to Figures 8 and 9). The temperature of the sintering sample is continuously monitored with an infrared pyrometer positioned a few meters directly above the sample surface. The high sintering rate of SPS technology limits surface reactions and suppresses particle grain development, hence enhancing its benefits. Research has demonstrated that SPS may efficiently remove surface oxides present at interparticle contact locations (Dibandjo *et al*., 2008). SPS has a cleaning effect on the particle surfaces of a material, as oxide formation is typically absent at the grain boundaries between the particles. The sporadic minute electric discharges occurring within the powder mass facilitate this. The spark plasma between neighbouring particles conducts heat produced by the pulsed current. The heat eliminates impurities from the powder's surface and melts and softens it, forming a neck that facilitates heat transfer by joule heating (see Figure 10). As the powder vaporizes at the microscopic level, the sintered sample will be devoid of contaminants (Groza & Zavaliangos, 2000; Jeje *et al*., 2021a). The SPS operation concludes with the cessation of the sintering process by reducing the furnace pressure and decreasing the temperature to ambient levels. Thereafter, the sintered samples are subjected to sandblasting to remove any excess graphite residue that may have stuck to them, in preparation for further examination or characterization (Matizamhuka, 2016; Abe *et al*., 2023).

The SPS method has recently attracted significant interest in materials science and processing, as it mitigates potential microstructural coarsening by facilitating shorter sintering durations through rapid heating rates and limited retention periods at sintering temperatures. Consequently, SPS is considered a genuine non-equilibrium processing method, unlike conventional PM technology. Grain boundary strengthening has been facilitated by the capability of SPS to rapidly and efficiently densify with minimum grain formation, hence enhancing the microstructure and improving the mechanical characteristics of several materials, including metals, ceramics, and polymers. SPS facilitates the development of composite materials with improved surface attributes, minimized defects, and superior densification, along with enhanced mechanical qualities such as elevated hardness and strength (Groza & Zavaliangos, 2000; Matizamhuka, 2016; Abe *et al*., 2020c; Kgoete *et al*., 2019; Cavaliere *et al*., 2019).

A recent study by Matizamhuka (2016), indicated that challenges in sustaining low grain growth rates, elevated melting points, prolonged dwell times at sintering temperatures, extensive powder surface areas, and detrimental chemical interactions with atmospheric gases (nitrogen, oxygen, and hydrogen) at high temperatures have significantly complicated conventional powder metallurgy sintering techniques. These factors make SPS more potent and better powder metallurgy technology. In another study on SPS published earlier by Zhang & co-workers (2013), it was

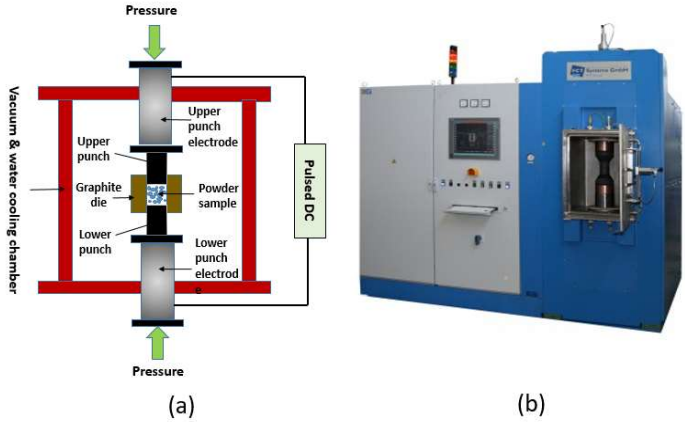

Figure 8: (a) Basic configuration of the SPS machine during sintering operation and (b) An automated SPS machine of model HHPD-25, FCT Systeme GmbH (Germany)

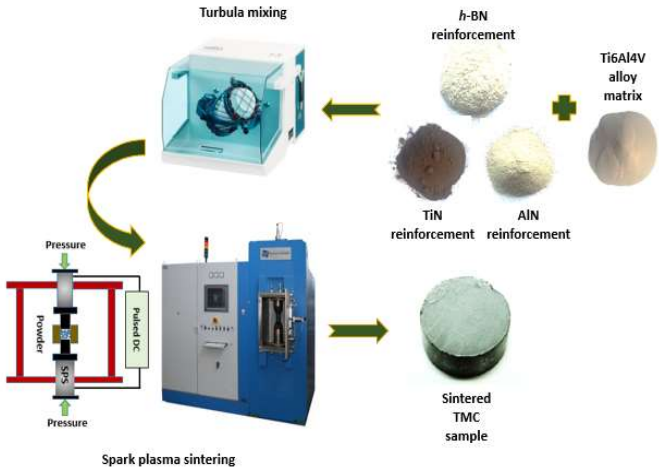

Figure 9: Depiction of spark plasma sintering of refractory nitride reinforced-TMC sample

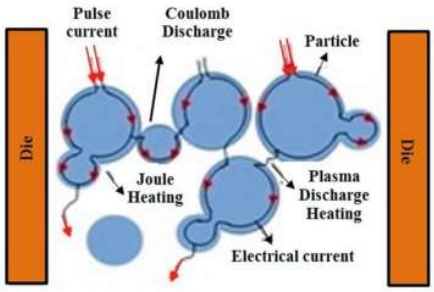

Figure 10: Mechanism of spark plasma sintering showing pulsed DC flow through the powder particles (Jeje *et al*., 2021a)

mentioned that when "ON/OFF" DC pulse voltage and current are applied to powders repeatedly, spark discharge and joule heating hotspots propagate across the entire sample as illustrated in Figure 10. The primary benefit SPS has over other more conventional sintering techniques is its ability to sinter materials fast, even those that are frequently difficult to sinter to full densification.

According to Garbiec *et al.* (2016), unlike traditional powder metallurgical procedures, the application of SPS facilitates the consolidation of diverse powders at reduced temperatures (ranging from 100 to 300 °C) within a relatively brief duration. The high efficiency achievable through the processing of diverse powders with the SPS technology is likely attributable to this factor. The authors indicated that quick densification and minimal grain growth within a brief timeframe for various powders, including metallic, ceramic, polymeric, and composite powders, elevate SPS above conventional hot-pressing technologies. Furthermore, the authors noted that researchers globally have investigated spark plasma sintered titanium and titanium-based composites, typically at temperatures between 700 and 1500 °C with compaction pressures from pressureless to 80 MPa. A heating rate of 100 °C/min and a holding duration of 2.5 to 20 minutes have been utilized. The authors investigated the influence of different heating rates and compaction pressures on the microstructure and mechanical properties of spark plasma sintered Ti6Al4V alloy, based on the data collected. The Ti6Al4V alloy powder with admixture was solidified at a temperature of 1000 °C. The microstructure, density, microhardness, elastic modulus, and compressive strength were examined about the simultaneous effects of varying sintering parameters, including compaction pressures of 5, 25, and 50 MPa, and heating rates of 200, 300, and 400 °C/min. The findings indicated that the parameters facilitated the creation of samples with a density between 4.14 and 4.43 g/cm^3, microhardness ranging from 293 to 373 HV0.05, elastic modulus from 116 to 142 GPa, and compressive strength between 1169 and 1414 MPa, respectively. The grain size grew with higher compaction pressure, and samples sintered at a compaction pressure of 50 MPa and a heating rate of 300 °C/min exhibited optimal results, with a microhardness of 373 HV0.05, an elastic modulus of 138 GPa, and a compressive strength of 1414 MPa.

C. Influences of Operational Parameters on Spark Plasma Sintering

The SPS process parameters determine its capability to synthesize titanium matrix composites to full densification. According to the research conducted by Diouf & Molinari (2012) and Ujah *et al.* (2019), the essential operating parameters in SPS include sintering temperature, compacting pressure, heating rate, and dwell time. The achievement of improved densification and superior thermal, physical, and mechanical qualities for the sintered compacts relies on these parameters. Consequently, it is essential to optimize these parameters to attain the highest quality of the sintered product while preserving finite time, energy, and material resources.

1) Influence of heating rate

The rapid heating rate achieved by SPS, capable of reaching 1000 °C/min, facilitates complete densification of the material while concurrently minimizing grain growth. In a research study, Shen *et al.* (2002) discovered that elevating the heating rate from 350 °C/min to 600 °C/min led to a reduction in alumina density. The researchers observed that an elevated heating rate led to a decrease in alumina particle size. In a comparable study, Lu *et al.* (2013) asserted that a quick heating rate is essential for the production of highly densified materials during SPS operation. Similarly, Qian *et al.* (2015) performed an experiment utilizing SPS to generate CP-Ti powder. Although the final density of the sintered material was minimally impacted, the authors claimed that the heating rate significantly influenced the densification process.

2) Influence of sintering pressure

The sintering pressure of a material typically progresses from a low to a medium and ultimately to a high value during SPS operation, leading to enhanced grain formation as the material's relative density increases. Likewise, an elevated microhardness value for the material may arise from augmented sintering pressure. Furthermore, the application of high pressure accelerates densification and promotes neck formation, which inhibits electric discharge and alters the joule effect via diffusion, resulting in the subsequent growth of grains (Garbiec *et al*., 2016).

3) Influence of sintering temperature

The sintering temperature employed in the fabrication of materials significantly influences the quality of the final sintered products during SPS. A higher sintering temperature often results in increased density of sintered materials. Garbiec *et al.* (2016) indicated that the Ti6Al4V alloy nearly attained complete densification at 1000 °C. Similarly, Falodun *et al.* (2018) observed that elevating the sintering temperature from 800 to 1000 °C led to a proportional enhancement in the relative density of the sintered titanium alloy, increasing from 97.29% to 99.54%.

4) Influence of holding time

The holding time is a significant operational factor in SPS. The holding time might affect the densification of the sintered material, thus influencing its mechanical properties. Yamanoglu *et al.* (2018) indicated that the holding duration

affected the relative density of Ti5Al2.5Fe alloys produced via SPS. It was found that an increase in holding time corresponded with an increase in the material's relative density.

VI. SPECIFIC REVIEW OF PUBLICATIONS IN THE OPEN LITERATURE ON REFRACTORY NITRIDE-REINFORCED TITANIUM-BASED COMPOSITES DEVELOPED BY SPS

A. *Review on the Characterization and Properties of Refractory Nitride-Reinforced Titanium Matrix Composites Developed by SPS*

Rominiyi *et al*. (2020) investigated the microstructural characterization, densification, and mechanical properties of sintered Ti–Ni–TiCN composites. Ti-Ni-TiCN composites with varying TiCN contents (5, 10, and 15 wt. %) were consolidated at a sintering temperature of 1100 °C for 10 minutes under vacuum conditions of less than 4 Pa, with a heating rate of 100 °C/min and an applied pressure of 50 MPa. The impact of Ni additive and TiCN nanoceramic reinforcement content on the densification, microstructure, and mechanical characteristics of the resulting composites was investigated. SEM was employed alongside EDS and XRD techniques to examine the morphology and phases present in the synthesized composites. The EDS and XRD data confirmed the presence of undissolved TiCN particles, in-situ generated TiN, and Ti_2Ni intermetallic phases. SEM analysis of the sintered composites revealed undissolved particles and lamellar topologies of phases within the matrix. With the increase in reinforcement material, the relative density of the sintered compacts decreased from 99.3% to 98.23%. It was found that an increase in the amount of reinforcement corresponded with an increase in the hardness of the sintered composites. The results of compression testing indicated that Ti-Ni-TiCN composites exhibited superior compressive strength compared to the pure Ti sample. The Ti-6Ni-10TiCN composite exhibited a Vickers hardness of 398 $HV_{1.0}$, with compressive yield and ultimate strengths of around 998 Pa and 1156 MPa, respectively, demonstrating superior properties.

Borkar *et al*. (2014) examined the effects of simultaneous in situ alloying and nitridation on sintered nitride-reinforced titanium-vanadium alloy composites. The authors combined elemental titanium and vanadium powders, using reactive nitrogen gas during SPS to fabricate a novel titanium-based composite material with nitride reinforcement. The resulting microstructure comprises δ-TiN phase precipitates with a NaCl structure, equiaxed (or globular) precipitates of a nitrogen-enriched hcp α(Ti,N) phase exhibiting a c/a ratio exceeding that of pure hcp Ti, and fine-scale plate-shaped precipitates of hcp α-Ti, dispersed within a bcc β matrix. Only the hcp α(Ti,N) and α-Ti phases manifest at reduced processing temperatures, while the δ-TiN phase forms at a temperature of 1400 °C during SPS processing. Consequently, composites fabricated at 1400 °C have the maximum microhardness, whereas those processed at 1300 °C or below demonstrate reduced values. The titanium and vanadium powder mixture experienced partial alloying when processed at temperatures below 1300 °C. The α(Ti,N) precipitates appear to encompass and maintain an orientation relationship with the nitride phase in the core, utilizing these δ-TiN precipitates as heterogeneous nucleation sites. Moreover, diminutive α-Ti plates develop within the nitride precipitates, perhaps due to the retrograde solubility of nitrogen in titanium.

Vasanthakumar *et al*. (2019) conducted a study on the synthesis and mechanical properties of TiC_x and Ti (C, N) reinforced titanium matrix in-situ composites manufactured via reactive SPS. This research involved ball-milling Ti powders with 2wt% graphene nanoplatelets (GnP) and graphitic carbon nitride (g-C_3N_4), followed by the fabrication of Ti-TiC_x and Ti–Ti (C, N) composites using SPS. The dispersion of GnP and g-C_3N_4 inside the Ti matrix was analysed post-milling. The research investigated the effects of GnP and g-C_3N_4 on the mechanical properties, phase evolution, and microstructure of the resultant composites. Ti (C, N) was identified in the Ti-2g-C_3N_4 sample, whereas the assessment of lattice parameters indicated the existence of the $TiC_{0.40}$ phase in the sintered compact of Ti-2GnP. Microstructural investigation indicated that Ti-2g-C_3N_4 exhibited a finer secondary phase compared to Ti-2GnP, attributable to the efficient dispersion of g-C_3N_4 in Ti during milling. Compared to other composites and pure titanium, Ti-2g-C_3N_4 exhibited superior Vickers hardness (820 ± 28 VHN), elastic modulus (168 GPa), nanohardness (12 GPa), room temperature compressive strength (2.9 GPa), and high-temperature compressive strength (120 MPa).

Diouf *et al*. (2017) fabricated pure titanium reinforced with titanium-based ceramic materials using SPS. Investigations were performed on the densification behaviour, microstructural changes, and hardness characteristics of commercially pure titanium (CP-Ti) with TiN, TiCN, TiC, and TiB_2 reinforcements during SPS. The CP-Ti powders were dry mixed for 5 hours at 49 rpm with varying weight percentages (2.5 and 5 wt. %) of ceramic additives in a T2F turbula mixer. The admixed composite powders were subsequently consolidated at 950 ºC, with a heating rate of 100 ºC/min and a dwell time of 5 minutes, utilizing a SPS equipment (model HHPD-25 from FCT Germany). Densification was monitored by examining punch displacement data and the density of the sintered sample by the Archimedes method. Incorporating 5% TiB_2 and 5% TiCN resulted in high densities of 97.8% and 99.6%, respectively, achieved at a relatively low temperature of 950 °C. Microstructural examinations suggest that the refined structure and homogeneous distribution of the reinforcements exert a growth-inhibiting impact on grains. All examined examples demonstrated an enhancement in hardness, with TiCN exhibiting the highest values attributable to the synergistic effects of TiC and TiN. The fracture mechanism transitioned from transgranular to intergranular.

Mutuk & Gürbüz (2021) examined the mechanical and wear characteristics of titanium composites reinforced with Si_3N_4, produced using SPS. The impact of different weight compositions (0–9 wt. %) of Si_3N_4 on the microstructure, density, hardness, and compressive strength of sintered titanium composites was examined. The mechanical characteristics were markedly enhanced with the addition of up to 3 wt. % Si_3N_4 following sintering at 1100°C for 120 minutes. In comparison to pure titanium (414.2 HV and 826 MPa), 3 wt. % Si_3N_4 reinforced composites exhibited superior hardness and compressive strength (698.5 HV and 1093 MPa). Compared to

pure titanium, the use of Si_3N_4 enhanced the wear characteristics of the sintered composites. The composite with 3 wt. % Si_3N_4 reinforcement exhibited the lowest wear rate, measuring $1.36x10^{-5}$, $2.75x10^{-5}$, and $5.15x10^{-5}$ mm³/Nm at loads of 10 N, 20 N, and 30 N, respectively. The SEM confirms a homogeneous dispersion of Si_3N_4 particles within the titanium matrix. The tendency of Si_3N_4 powder to agglomerate resulted in a decline in the properties of the composites beyond this ratio. The XRD phase analysis revealed the absence of any in-situ generated secondary phases inside the composite structure.

Bustillos *et al*. (2020) conducted a study on titanium composites reinforced with 1 wt. % boron nitride nanotubes (BNNTs) using SPS. This study investigated the feasibility of fabricating Ti-BNNT composites at low temperature and high pressure conditions. This study aims to solve two concerns concerning the performance of BNNT–metal matrix composites: the dispersion of high-surface-energy BNNTs using an ultrasonic-assisted method and the management of reactions at the metal/nanotube interface. Sintering at low (750 °C and 555 MPa) and high (950 °C and 60 MPa) temperature conditions yielded relative densities of 97% and 99%, respectively, whereas high-energy ultrasonic vibrations effectively dispersed entangled BNNTs. Brittle interfacial products can be reduced by sintering at temperatures up to 35% lower than those employed in conventional sintering. Furthermore, the rapid densification (10 minutes) achieved with the SPS approach restricts the range of reactions for composites sintered at elevated temperatures and low pressure (TiB_2, TiB). The composites exhibit yield strength enhancements of 46% and 50%, respectively, compared to the Ti alloy, when sintered at low and high temperatures. The composite materials demonstrate the capacity to impede plasticity in the presence of BNNTs, reaction phases, and twin boundaries that pin dislocations, as evidenced by their strain hardening exponents of 0.8 and 0.5.

Jeje *et al*. (2021b) conducted a research on the development and characterization of a Ti7Al1Mo composite reinforced with TiN nanoceramic by SPS. This work investigated the impact of TiN nanoparticle reinforcement on the densification, microstructural evolution, and mechanical properties of the Ti7Al1Mo ternary alloy. The unreinforced Ti7Al1Mo alloy had a microstructure characterized by distinct grain boundaries and a Widmanstätten lath-like shape, containing minimal beta (β) phase and mostly alpha (α) phase. The morphology of the nano-TiN reinforced Ti7Al1Mo composites exhibited a bimodal structure. Upon comparison of the Ti7Al1Mo/7TiN composite with the unreinforced Ti7Al1Mo ternary alloy, it was determined that the composite exhibits a maximum compressive yield strength of 1295 ± 7 MPa and a peak hardness of 549 ± 22 HV1.0, reflecting enhancements of 74 HV and 323 MPa, respectively. The developed composites exhibited significant potential for load-bearing applications.

Falodun *et al*. (2019) performed a study on the characterization of nano-TiN reinforced titanium fabricated using SPS, utilizing EBSD and TKD techniques. The study investigated the impact of dispersion behaviour, interface reactions, and the incorporation of ceramic nanoparticles on the sintered titanium matrix composite. The microstructural examination of the sintered composite was performed using transmission Kikuchi diffraction (TKD), electron backscatter diffraction (EBSD) with field emission scanning electron microscopy (FE-SEM), and X-ray diffraction (XRD) for phase identification. The results indicate that TiN nanoparticles were evenly dispersed inside the sintered composite, resulting in the formation of grains with modified crystallographic orientations after the incorporation of nanoparticle material. Additionally, TKD revealed the development of TiN interface sub-grain structures at the grain boundary during the SPS process.

B. Review on the Characterization and Properties of Refractory Nitride-Reinforced Ti6Al4V Matrix Composites Developed by SPS

Kgoete *et al*. (2018a) conducted a study on the effects of silicon nitride (Si_3N_4) on the microstructure, corrosion resistance, and thermal stability of Ti6Al4V matrix composites fabricated using SPS. The sintering occurred at 1000 °C for a duration of 6 minutes at a pressure of 50 MPa. Various weight ratios of Si_3N_4 powder were combined with Ti6Al4V powder. The composite mixture was utilized to produce the sintered samples, which were subsequently analysed for their mechanical and thermal properties, along with the influence of Si_3N_4 on the microstructure. The overall morphology of the sintered composites was examined using a scanning electron microscope (SEM-EDS). The energy dispersive X-ray diffraction spectrometer (EDXS) was employed to analyse the phases contained in the fabricated sintered composites. Microhardness was analysed using a high-impact diamond Durascan microhardness tester. The potentiodynamic polarization technique was employed to evaluate the electrochemical behaviour of the sintered samples. A thermal gravimetric analyser (TGA) was employed to assess the thermal characteristics of sintered composites. The experimental data indicate that the incorporation of Si_3N_4 enhanced the material's microstructure, corrosion resistance, and thermal stability properties. The reinforcement demonstrated a beneficial effect on the performance attributes of the Ti6AI4V alloy in aerospace applications, according to the authors.

Abe *et al*. (2023) evaluated the nanomechanical and tribological properties of Ti6Al4V alloy matrix composites reinforced with refractory nitride, produced using SPS. The authors investigated the effects of single (3 wt. % each) and double (1.5 wt. % each) nanoparticles of hexagonal boron nitride, titanium nitride, and aluminium nitride reinforcements on the phase composition, microstructure, nanomechanical properties, and tribological characteristics of the sintered TMCs. The examination of the microstructure and phase demonstrated that sintered TMCs exhibit no visible defects or harmful intermetallic phases, suggesting the absence of adverse particle-matrix interfacial reactions during the sintering process. The outcomes of nanoindentation and tribology assessments on sintered TMCs showed notable enhancements in hardness, elastic modulus, and wear resistance across all reinforcing types.

Falodun *et al*. (2017) examined the influence of SPS temperature and duration on TiN nanoparticle-reinforced

Ti6Al4V matrix composites. In a T2F Turbula mixer, Ti6Al4V particles and nano-TiN were combined in different proportions (1-4 vol. %). The blended powders were consolidated utilizing SPS. The sintered compacts were analysed using field emission scanning electron microscopy (FE-SEM) integrated with energy dispersive X-ray spectroscopy (EDS) and X-ray diffractometry techniques. Investigations were conducted on the microindentation hardness and fracture behaviour of the sintered compacts. The findings indicate that elevating the sintering temperature significantly affects the relative densities of the composites, ranging from 97% to 99%, and their microhardness, increasing from 389 $HV_{0.1}$ to 602 $HV_{0.1}$. The incorporation of TiN resulted in the transformation of the lamellar α/β phases in Ti6Al4V into duplex (bimodal) structures, as evidenced by the microstructural investigations. The fracture morphology of the sintered alloys exhibits a transgranular pattern with fine dimple features that enhance the cohesiveness and strength of the grains, while the sintered composite held for 30 minutes demonstrates the highest microhardness value, primarily influenced by the presence of the Ti_2N phase.

Kgoete *et al*. (2018b) examined the impact of reinforcing materials and the SPS process on the microstructure, densification, microhardness, and corrosion behaviour of Ti6Al4V-Si_3N_4 composites. The Si_3N_4 reinforcement was added in different proportions (5–15 wt. %) within the Ti6Al4V alloy matrix. The SPS method was subsequently employed to effectively consolidate the composite powders. SEM examination of the sintered composites showed the dual α/β phase microstructures of Ti6Al4V and the distribution of Si_3N_4 particles inside the matrix. XRD examination of the composites revealed an increased intensity of the diffraction peaks corresponding to the Si_3N_4 phase while microhardness increased from 325.46 $HV_{0.1}$ to 585.73 $HV_{0.1}$ with increasing reinforcement concentration. The use of Si_3N_4 improved the corrosion resistance of the sintered composite, decreasing it from 0.986629 mm/year to 0.030547 mm/year.

Abe *et al*. (2020c) conducted a study examining the effects of aluminium nitride (AlN) and hexagonal boron nitride (*h*-BN) nano-reinforcements on the microstructure, phase composition, hardness, and oxidation resistance of Ti6Al4V-based composites. The synthesized powders underwent sintering via spark plasma sintering (SPS), an advanced technology that facilitates rapid heating and cooling. Subsequently, the microstructure and phase compositions were analysed through scanning electron microscopy, optical microscopy, and X-ray diffractometry; densification was evaluated via Archimedes' principle; hardness values were measured using the Vickers microhardness test; and the oxidation resistance of the sintered composites was investigated through thermogravimetric analysis. The maximum relative densification value of 99.77% was achieved with a uniform mixture of nano-reinforcements comprising 1.5 wt. % each of AlN and *h*-BN. The hardness value of Ti6Al4V-1.5AlN-1.5*h*-BN (656.01 HV) was inferior to that of Ti6Al4V-3*h*-BN (716.80 HV), suggesting that the phase compositions within the microstructure significantly influence the hardness characteristics of the composites, surpassing the effects of standard relative densification. Ti6Al4V-1.5AlN-1.5*h*-BN had the greatest resistance to oxidative heat in air, with the minimal positive weight change of 0.36 mg/cm².

Falodun *et al*. (2018) examined the influence of SPS and TiN reinforcement on the densification, microstructure, microhardness, and wear behaviour of Ti6Al4V matrix composites. SPS was effectively employed to fabricate Ti6Al4V/TiN composites. The volume percentage of TiN added to Ti6Al4V was altered from 1% to 5%. The authors indicate that with the addition of TiN, the density of the sintered samples decreased from 99% to 97%, however the microhardness value rose from 389 $HV_{0.1}$ to 488 $HV_{0.1}$. An advanced α/β phase microstructure in Ti6Al4V, characterized by evenly distributed TiN particles, was identified through SEM analysis of SPS-sintered nanocomposites. The authors determined that the Ti6Al4V/TiN composite was effectively fabricated using spark plasma sintering (SPS), and its wear surface exhibited enhanced abrasion resistance with discontinuous grooves in contrast to the sintered pure Ti6Al4V matrix.

Kgoete *et al*. (2019) conducted a work focused on examining the high-temperature oxidation of Ti6Al4V-TiN composites fabricated using SPS. The samples included in the investigation were fabricated via the spark plasma sintering technique at 1000 °C for 6 minutes under a pressure of 50 MPa. The alloy was mixed with varying quantities of TiN, ranging from 5 to 15 wt. %, and the effects of the ceramic additions on the samples subjected to thermal gravimetric measurement were investigated. The formation of the oxide layer on the samples' surfaces was examined using SEM-EDS. Energy dispersive X-ray diffraction spectroscopy was employed to identify the phases in the oxidized samples. A high-impact diamond DuraScan microhardness tester was employed to examine microhardness parameters. The thermal gravimetric analyser (TGA) was employed to investigate Ti6Al4V and Ti6Al4V-xTiN composites in air within the temperature range of 45-800 °C. The results indicated that the oxidation resistance and hardness of the Ti6Al4V alloy were significantly improved by TiN reinforcement, making it beneficial for aerospace applications. The Ti6Al4V alloy, reinforced with 5 wt. % TiN, exhibited an increased hardness value of 881.15 HV and minimal weight gain, indicating superior resistance to high-temperature oxidation.

Abe *et al*. (2022) carried out a study on the nanomechanical and tribological properties of Ti6Al4V alloy matrix composites reinforced with varying concentrations (1, 3, and 5 wt. %) of hexagonal boron nitride, generated using SPS. This study examined the microstructural and phase constituents of the sintered TMCs using optical microscopy, energy-dispersive X-ray spectroscopy, and scanning electron microscopy/diffraction. An automated nanoindenter with a maximum load of 200 mN and a pin-on-disk tribometer with applied loads of 5, 10, and 15 N were utilized for the tribology experiment and nanoindentation, respectively. SPS was shown to enhance the development of highly densified products, finely refined grains, and a robust interfacial bond between the matrix and reinforcement. Furthermore, it was demonstrated that an increase in *h*-BN reinforcement content resulted in improved tribological properties of the TMCs, alongside enhancements in nanoindentation hardness (50.66 ± 2.25-

70.78 ± 3.34 GPa) and modulus of elasticity (238.69 ± 12.25-356.76 ± 21.34 GPa).

Maja *et al*. (2018) conducted nanoindentation investigations on a Ti6Al4V matrix composite reinforced with TiN nanoceramics. This study employed the ultra-nanoindenter (UNHT) technique to investigate the mechanical characteristics of Ti6Al4V composites reinforced with 1-4 vol% TiN. The addition of reinforcements enhances the mechanical properties of sintered compacts by regulating the grain morphology of the microstructure. Furthermore, the nanoindentation results unequivocally shown that the incorporation of TiN into the Ti6Al4V matrix enhances both hardness and modulus of elasticity. In comparison to the Ti6Al4V alloy, the sample with 4 vol. % TiN had the highest indentation hardness of 7517 MPa (696 HV) and an elastic modulus of 156 GPa. Furthermore, sintered nanocomposite materials exhibited enhanced wear resistance relative to the Ti6Al4V alloy and demonstrated greater hardness alongside a reduction in maximum indentation depth.

Kgoete *et al*. (2018c) examined the effects of microsized Si_3N_4 and TiN ceramic additives on the microstructure and mechanical properties of spark plasma sintered Ti-6Al-4V-Si_3N_4-TiN ternary composites for aerospace applications. Spark plasma sintering was conducted at a temperature of 1000 °C, a pressure of 50 MPa, and a duration of 6 minutes. Systematic consolidation was performed on various ceramic additions comprising 2.5 wt. % Si_3N_4-2.5 wt. % TiN, 5 wt. % Si_3N_4-5 wt. % TiN, and 7.5 wt. % Si_3N_4-7.5 wt. % TiN, along with Ti6Al4V and Ti6Al4V-Si_3N_4-TiN powders. The influence of several ceramic additives on the microstructure, phase composition, and mechanical properties of spark plasma sintered composites was evaluated using SEM-EDS, XRD, and a diamond Dura scan microhardness tester. The electrochemical behaviour of the sintered samples was evaluated using a potentiodynamic polarization approach in a solution of 0.1M HCl and 3.65% NaCl. The experimental results indicated that the incorporation of Si_3N_4 and TiN improved the microstructure, hardness, and corrosion resistance properties of the spark plasma sintered composites. Furthermore, Si_3N_4 and TiN demonstrated a beneficial effect on the performance attributes of the Ti6Al4V alloy.

VII. CONCLUSION

This review has provided a comprehensive overview of titanium, its alloys, titanium matrix composites (TMCs), and refractory nitride reinforcements, with an emphasis on classifications, processing routes, and material properties. A particular focus has been placed on spark plasma sintering (SPS) as a promising powder metallurgy technique for the consolidation of TMCs, owing to its ability to achieve rapid densification, refined microstructures, and enhanced mechanical performance. Titanium alloys remain widely used in aerospace due to their high specific strength and corrosion resistance; however, their broader adoption is limited by drawbacks such as low hardness, poor wear resistance, and thermal degradation at elevated temperatures. These shortcomings have stimulated growing interest in reinforcing titanium matrices with advanced ceramics, particularly refractory nitrides, to develop high-performance composites.

Refractory nitrides such as TiN, h-BN, Si_3N_4, and AlN offer a unique combination of high hardness, thermal stability, chemical resistance, and structural integrity at elevated temperatures. When integrated into TMCs and processed via SPS, these reinforcements significantly enhance the composites' mechanical and thermal properties, making them attractive for aerospace and other high-demand applications. Nonetheless, critical challenges remain in terms of optimizing SPS parameters such as sintering temperature, pressure, heating rate, and dwell time, to maximize performance while minimizing resource use. Furthermore, the high cost of TMC production must be addressed to facilitate broader industrial adoption.

A key gap in the current literature lies in the limited exploration of diverse refractory nitride combinations including binary, ternary, or quaternary, as reinforcements for TMCs. This represents a promising direction for future research, with potential to yield novel materials suited not only for aerospace applications but also for the electronics, automotive, and energy sectors, where advanced thermal and mechanical properties are increasingly required..

AUTHORS' CONTRIBUTIONS

J. O. Abe: Conceptualization; Visualization; Investigation; Methodology; Data curation; Writing-original draft. **O. M. Popoola:** Conceptualization; Supervision; Fund acquisition; and Writing - review & editing. **A. P. I. Popoola**: Conceptualization; Supervision; Project administration; and Resources.

ACKNOWLEDGMENT

This work is based on the research supported wholly/in part by the National Research Foundation of South Africa (Grant Numbers: 150574); and Tshwane University of Technology - Faculty of Engineering and Built Environment, Centre for Energy and Electric Power and Surface Engineering Research Laboratory (SERL) under the Leadership of Professor API Popoola.

REFERENCES

Abe, J.; Popoola, O.; and Popoola, P. (2024a). Investigating the Mechanical Properties of Spark Plasma-Sintered Refractory Nitride-Reinforced Titanium Alloy Matrix Composites for Energy-Saving High-Temperature Aerospace Application. Paper presented at the 9th North American Conference on Industrial Engineering and Operations Management (IEOM 2024), Washington, DC, USA.

Abe, J. O.; Popoola, A. P. I. and Popoola, O. M. (2019a). Influence of Varied Process Parameters on the Microstructure, Densification, and Microhardness of Spark Plasma Sintered Ti-6Al-4V/h-BN Binary Composite. Paper presented at the 6th International Conference on Mechanical, Materials and Manufacturing (ICMMM 2019), Boston, USA.

Abe, J. O.; Popoola, A. P. I. and Popoola, O. M. (2020a). Consolidation of Ti6Al4V Alloy and Refractory Nitride Nanoparticles by Spark Plasma Sintering Method: Microstructure, Mechanical, Corrosion and Oxidation Characteristics. Materials Science and Engineering: A, 774:138920.

Abe, J. O.; Popoola, A. P. I.; Popoola, O. M. and Ajenifuja, E. (2020b). Effects of Refractory Nitride Reinforcements on the Microstructure, Densification, and Microhardness of Ti6Al4V-Based Binary Composites Produced by Spark Plasma Sintering. Paper presented at the 2nd International Conference on Mechanical Manufacturing and Industrial Engineering (MMIE 2019), Beijing, China.

Abe, J. O.; Popoola, A. P. I.; Popoola, O. M. and Ajenifuja, E. (2020c). Microstructural, Phase, Hardness, and Oxidation Resistance Studies of AlN/*h*-BN-Reinforced Ti6Al4V Matrix Composites Synthesized by Spark Plasma Sintering. The International Journal of Advanced Manufacturing Technology, 107:2985-2994.

Abe, J. O.; Popoola, O. M. and Popoola, A.P. (2023). Assessment of Nanomechanical and Tribological Performance of Refractory Nitride-Reinforced Titanium Alloy Matrix Composites Developed by Spark Plasma Sintering. The Journal of the Minerals, Metals and Materials Society, 75(3):791-805.

Abe, J. O.; Popoola, O. M. and Popoola, P. A. (2022). Nanomechanical and Tribological Properties of Hexagonal-Boron Nitride-Enhanced Sintered Titanium Alloy Matrix Composites. Paper presented at the 23rd Annual International RAPDASA Conference joined by RobMech, PRASA and CoSAAMI, Cape Town, South Africa.

Abe, J. O.; Popoola, O. M. and Popoola, P. A. (2024b). A synergetic effect of ternary refractory nitride reinforcements on densification, mechanical, tribological and thermal stability characteristics of spark plasma sintering-developed Ti6Al4V matrix composites. Journal of Alloys and Compounds, 997, 174888.

Abe, J. O.; Popoola, O. M.; Popoola, A. P. I.; Ajenifuja, E. and Adebiyi, D. I. (2019b). Application of Taguchi design method for optimization of spark plasma sintering process parameters for Ti-6Al-4V/h-BN binary composite. Engineering Research Express, 1(2), 025043.

Adegbenjo, A. O.; Nsiah-Baafi, E.; Shongwe, M. B.; Olubambi, P. A. and Potgieter, J. H. (2017). Low Temperature Spark Plasma Sintered Irregular Shaped Ti6Al4V Powders with Enhanced Properties. Journal of Engineering Technology, 6(1):35-48.

Adegbenjo, A. O.; Obadele, B. A. and Olubambi, P. A. (2018). Densification, Hardness and Tribological Characteristics of MWCNTs Reinforced Ti6Al4V Compacts Consolidated by Spark Plasma Sintering. Journal of Alloys and Compounds, 749:818-833.

Ajay, C. V.; Hariharasakthisudhan, P.; Vinoth, V. and Sundaravignesh, S. (2023). Influence of process parameters on the tribological behaviour of dual reinforcement (Al_2O_3/Si_3N_4) in AA6061 metal matrix composite. Materials Today: Proceedings.

Akinwamide, S. O.; Obadele, B. A.; Adams, F. V. and Olubambi, P. A. (2020). Microstructure and Corrosion Response of Spark-Plasma-Sintered 304 Austenitic Stainless Steel Reinforced with Titanium Nitride in Chloride Environments. Journal of Failure Analysis and Prevention, 20, 833-842.

Akinwamide, S. O.; Tshabalala, N.; Falodun, O. E.; Oke, S. R.; Akinribide, O. J.; Abe, B. T. and Olubambi, P. A. (2019). Microstructural and corrosion resistance study of sintered Al-TiN in Sodium Chloride solution. Materials Today: Proceedings, 18, 2881-2886.

Al Islam, W. and Rahman, M. (2021). A Review on Types and Properties of Advanced Composite Materials for Aerospace Applications. Paper presented at the 5th Annual International Conference on Mechanical Engineering and Renewable Energy (ICMERE), Chattogram, Bangladesh.

Al-Aqeeli, N. (2013). Processing of CNTs Reinforced Al-Based Nanocomposites Using Different Consolidation Techniques. Journal of Nanomaterials, 2013:125-125.

Alavala, C. R. (2016). Effect of Thermoelastic Behavior on interfacial debonding and Particulate Fracture in AA1100/TiN Nanoparticulate Metal Matrix Composites. International Journal of Science and Research, 5(3), 1295-1300.

Anderson, R.E., 1998. Titanium matrix composite turbine engine component consortium (TMCTECC). Advanced Materials and Process Technology Information Analysis Center (AMPTIAC) Newsletter, Winter.

Aydin, F. and Turan, M. E. (2020). The effect of boron nitride on tribological behavior of Mg matrix composite at room and elevated temperatures. Journal of Tribology, 142(1), 011601.

Ayodele, O. O.; Awotunde, M. A.; Babalola, B. J. and Olubambi, P. A. (2021). Spark plasma sintering of CNT-NiAl nanocomposites–Process parameter, densification mechanism, and grain analysis. Manufacturing Review, 8, 25.

Ayodele, O. O.; Babalola, B. J. and Olubambi, P. A. (2023). Evaluation of the wear and mechanical properties of titanium diboride-reinforced titanium matrix composites prepared by spark plasma sintering. Materials, 16(5), 2078.

Bai, M.; Namus, R.; Xu, Y.; Guan, D.; Rainforth, M. W. and Inkson, B. J. (2019). In-situ Ti-6Al-4V/TiC Composites Synthesized by Reactive Spark Plasma Sintering: Processing, Microstructure, and Dry Sliding Wear Behaviour. Wear, 432:202944.

Balaji, V. S. and Kumaran, S. (2015). Dry Sliding Wear Behaviour of Titanium-(TiB+ TiC) in Situ Composite Developed by Spark Plasma Sintering. Tribology Transactions, 58(4):698-703.

Balasubramanian, M. 2013. Composite Materials and Processing (1st ed.). CRC Press, Taylor & Francis Group Publisher, Boca Raton, Florida, USA.

Baturina, T. I.; Mironov, A. Y.; Vinokur, V. M.; Baklanov, M. R. and Strunk, C. (2007). Localized superconductivity in the quantum-critical region of the disorder-driven superconductor-insulator transition in TiN thin films. Physical review letters, 99(25), 257003.

Berger, L. I. (2020). Semiconductor Materials. CRC Press, Taylor & Francis Group Publisher, Oxfordshire, UK**.**

Bewlay, B. P.; Nag, S.; Suzuki, A. and Weimer, M. J. (2016). TiAl alloys in commercial aircraft engines. Materials at High Temperatures, 33(4-5), 549-559.

Bhattacharya, N.; Unde, J. and Kulkarni, K. (2020). Use of Titanium and its Alloy in Aerospace and Aircraft Industries. International Journal of Creative Research Thoughts, 8:1383-1396.

Biswas, A. and Majumdar, J. D. (2009). Surface Characterization and Mechanical Property Evaluation of Thermally Oxidized Ti-6Al-4V. Material Characterization, 513-518.

Borkar, T.; Nag, S.; Ren, Y.; Tiley, J. and Banerjee, R. (2014). Reactive Spark Plasma Sintering (SPS) Of Nitride Reinforced Titanium Alloy Composites. Journal of Alloys and Compounds, 617:933-945.

Boyer, R. R. (1996). An Overview on the Use of Titanium in the Aerospace Industry. Materials Science and Engineering: A, 213(1-2):103-114.

Brice, D. A.; Samimi, P.; Ghamarian, I.; Liu, Y.; Brice, R. M.; Reidy, R. F. and Collins, P. C. (2016). Oxidation Behavior and Microstructural Decomposition of Ti-6Al-4V and Ti-6Al-4V-1B Sheet. Corrosion Science, 112:338–346.

Bustillos, J.; Lu, X.; Nautiyal, P.; Zhang, C.; Boesl, B. and Agarwal, A. (2020). Boron nitride nanotube–reinforced titanium composite with controlled interfacial reactions by spark plasma sintering. Advanced Engineering Materials, 22(12), 2000702.

Callister, W. D. and Rethwisch, D. G. (2015). Materials Science and Engineering: An Introduction. Hoboken, John Wiley & Sons, Inc. Publisher, New Jersey, USA.

Cao, Y.; Zeng, F.; Lu, J.; Liu, B.; Liu, Y. and Li, Y. (2015). In situ synthesis of TiB/Ti6Al4V composites reinforced with nano TiB through SPS. Materials Transactions, 56(2), 259-263.

Cavaliere, P.; Sadeghi, B. and Shabani, A. (2019). Spark Plasma Sintering: Process Fundamentals. Spark Plasma Sintering of Materials: Advances in Processing and Applications, 3-20.

Chand, S. and Chandrasekhar, P. (2020). Influence of B4C/BN on solid particle erosion of Al6061 metal matrix hybrid composites fabricated through powder metallurgy technique. Ceramics International, 46(11), 17621-17630.

Chandran, K. R. and Panda, K. B. (2002). Titanium composites with TiB whiskers. Advanced Materials & Processes, 160(10), 59-63.

Chasnyk, V. I.; Chasnyk, D. V.; Fesenko, I. P. and Kaidash, O. M. (2020). A Study of the Thermal Conductivity, Electrical Resistivity, and Microwave Absorption of Pressureless Sintered AlN–Y_2O_3–Mo and AlN–Y_2O_3–TiN Composites. Journal of Superhard Materials, 42, 165-176.

Chen, L.; Lü, S. L.; Zhao, D. J.; Guo, W.; Li, J. Y. and Wu, S. S. (2023). Progress in preparation of AlN-reinforced magnesium matrix composites: A review. China Foundry, 1-10.

Chen, Y. C. and Ou, S. F. (2020). Effects of Reinforcement Ratios and Sintering Temperatures on the Mechanical Properties of Titanium Nitride/Nickel Composites. Materials, 13(20), 4473.

Cheng, Z.; Koh, Y. R.; Mamun, A.; Shi, J.; Bai, T.; Huynh, K.; Yates, L.; Liu, Z.; Li, R.; Lee, E. and Liao, M. E. (2020). Experimental observation of high intrinsic thermal conductivity of AlN. Physical Review Materials, 4(4), 044602.

Çiftçi, N. O. (2013). Chemical vapor deposition of boron nitride nanotubes. Master's Thesis, Bilkent Universitesi, Turkey.

Dai, J.; Zhu, J.; Chen, C. and Weng, F. (2016). High Temperature Oxidation Behaviour and Research Status of Modifications on Improving High Temperature Oxidation Resistance of Titanium Alloys and Titanium Aluminides: A Review. Journal of Alloys and Compounds, 685:784-798.

Dancy, G. S.; Sheeba, V. B.; Louis, C. N. and Amalraj, A. (2015). Superconductivity in Group III-V Semiconductor AlN Under High Pressure. Orbital: The Electronic Journal of Chemistry, 226-230.

Delbari, S. A.; Namini, A. S. and Asl, M. S. (2019). Hybrid Ti matrix composites with TiB2 and TiC compounds. Materials Today Communications, 20, 100576

Dhinakarraj, C. K.; Senthilkumar, N.; Palanikumar, K. and Deepanraj, B. (2023). Experimental interrogations on morphologies and mechanical delineation of silicon nitride fortified Mg-Al-Zn alloy composites. Materials Today Communications, 35, 105731.

Dibandjo, P.; Bois, L.; Estournes, C.; Durand, B. and Miele, P. (2008). Silica, Carbon, and Boron Nitride Monoliths with Hierarchical Porosity Prepared by Spark Plasma Sintering Process. Microporous and Mesoporous Materials, 111(1-3):643-648.

Diouf, S. and Molinari, A. (2012). Densification Mechanisms in Spark Plasma Sintering: Effect of Particle Size and Pressure. Powder Technology, 221:220-227.

Diouf, S.; Durowoju, M. O.; Shongwe, M. B. and Olubambi, P. A. (2017). Processing of Pure Titanium Containing Titanium-Based Reinforcing Ceramics Additives Using Spark Plasma Sintering. Leonardo Electronic Journal of Practical Technology, 30:269-286.

Donachie, M. J. (2000). Titanium: A Technical Guide. ASM International Publisher, Michigan, USA.

Dow, H. S.; Kim, W. S. and Lee, J. W. (2017). Thermal and electrical properties of silicon nitride substrates. AIP Advances, 7(9).

Duan, X.; Jia, D.; Wang, Z.; Cai, D. T.; Yang, Z.; He, P.; Wang, S. and Zhou, Y. (2016). Influence of hot-press sintering parameters on microstructures and mechanical properties of h-BN ceramics. Journal of Alloys and Compounds 684, 474-480.

Eichler, J. and Lesniak, C. (2008). Boron nitride (BN) and BN composites for high-temperature applications. Journal of the European Ceramic Society, 28(5), 1105-1109.

Emura, S.; Hagiwara, M. and Yang, S. J. (2004). Room-temperature tensile and high-cycle-fatigue strength of fine TiB particulate-reinforced Ti-22Al-27Nb composites. Metallurgical and Materials Transactions A, 35, 2971-2979.

Ertuğ, B. (2013). Powder Preparation, Properties and Industrial Applications of Hexagonal Boron Nitride. Sintering Applications, 33-56.

Falcon-Franco, L.; Rosales, I.; García-Villarreal, S.; Curiel, F. F. and Arizmendi-Morquecho, A. (2016). Synthesis of magnesium metallic matrix composites and the evaluation of aluminum nitride addition effect. Journal of Alloys and Compounds, 663, 407-412.

Fale, S.; Likhite, A. and Bhatt, J. (2015). Compressive, tensile and wear behavior of ex situ Al/AlN metal matrix nanocomposites. Journal of Composite Materials, 49(16), 1917-1928.

Falodun, O. E.; Obadele, B. A.; Oke, S. R.; Ige, O. O.; Olubambi, P. A.; Lethabane, M. L. and Bhero, S. W. (2018). Influence of Spark Plasma Sintering on Microstructure and Wear Behaviour of Ti-6Al-4V Reinforced with Nanosized TiN. Transactions of Nonferrous Metals Society of China, 28(1):47-54.

Falodun, O. E.; Obadele, B. A.; Oke, S. R.; Maja, M. E. and Olubambi, P. A. (2017). Synthesis of Ti-6Al-4V Alloy with Nano-TiN Microstructure via Spark Plasma Sintering Technique. Presented at the 4th International Conference on Mechanical, Materials and Manufacturing (*ICMMM 2017*), Atlanta, Georgia, USA.

Falodun, O. E.; Obadele, B. A.; Oke, S. R.; Olubambi, P. A. and Westraadt, J. (2019). Characterization of spark plasma sintered TiN nanoparticle strengthened titanium alloy using EBSD and TKD. Materials Research Bulletin, 117, 90-95.

Falodun, O. E.; Oke, S. R.; Olubambi, P. A.; Dirisu, J. O. and Sule, R. (2023). Microstructural Characteristics and Wear Behavior of Sintered Ni-Modified Ti–x TiB_2 Composites. Journal of The Institution of Engineers (India): Series D, 1-10.

Fayomi, J.; Popoola, A. P. I.; Popoola, O. M.; Oladijo, O. P. and Fayomi, O. S. I. (2020). Understanding the microstructural evolution, mechanical properties, and tribological behavior of AA8011-reinforced nano-Si_3N_4 for automobile application. The International Journal of Advanced Manufacturing Technology, 111, 53-62.

Feng, H.; Zhou, Y.; Jia, D. and Meng, Q. (2004). Microstructure and mechanical properties of in situ TiB reinforced titanium matrix composites based on Ti–FeMo–B prepared by spark plasma sintering. Composites Science and Technology, 64(16), 2495-2500.

Firestein, K. L.; Corthay, S.; Steinman, A. E.; Matveev, A. T.; Kovalskii, A. M.; Sukhorukova, I. V.; Golberg, D. and Shtansky, D. V. (2017). High-strength aluminum-based composites reinforced with BN, AlB2 and AlN particles fabricated via reactive spark plasma sintering of Al-BN powder mixtures. Materials Science and Engineering: A, 681, 1-9.

Franczak, A. and Karwan-Baczewska, J. (2017). Copper matrix composites reinforced with titanium nitride particles synthesized by mechanical alloying and spark plasma sintering. Metallurgy and Foundry Engineering, 43(2), 97-105.

Gao, C.; Wang, Z.; Xiao, Z.; You, D.; Wong, K. and Akbarzadeh, A. H. (2020). Selective laser melting of TiN nanoparticle-reinforced AlSi10Mg composite: Microstructural, interfacial, and mechanical properties. Journal of Materials Processing Technology, 281, 116618.

Garbiec, D.; Leshchynsky, V.; Colella, A.; Matteazzi, P. and Siwak, P. (2019). Structure and Deformation Behavior of Ti-SiC Composites Made by Mechanical Alloying and Spark Plasma Sintering. Materials, 12(8):1276.

Garbiec, D.; Siwak, P. and Mróz, A. (2016). Effect of Compaction Pressure and Heating Rate on Microstructure and Mechanical Properties of Spark Plasma Sintered Ti6Al4V Alloy. Archives of Civil and Mechanical Engineering 16, 702-707.

Geng, K.; Lu, W.; Qin, Y. and Zhang, D. (2004). In situ preparation of titanium matrix composites reinforced with TiB whiskers and Y_2O_3 particles. Materials research bulletin, 39(6), 873-879.

Gorsse, S. and Miracle, D.B. (2003). Mechanical properties of Ti-6Al-4V/TiB composites with randomly oriented and aligned TiB reinforcements. Acta Materialia, 51(9), 2427-2442.

Gospodinov, D.; Ferdinandov, N. and Dimitrov, S. (2016). Classification, Properties and Application of Titanium and its Alloys. Proceedings of University of Ruse, 55(2):27-32.

Groza, J.R. and Zavaliangos, A. (2000). Sintering activation by external electrical field. Materials Science and Engineering: A, 287(2), 171-177.

Guleryuz, H. and Cimenoglu, H. (2009). Oxidation of Ti–6Al–4V Alloy. Journal of Alloys and Compounds, 472(1-2):241-246.

Hampshire, S. (2007). Silicon nitride ceramics–review of structure, processing and properties. Journal of achievements in materials and manufacturing engineering, 24(1), 43-50.

Hanumantharayappa, A. K. B.; Prasanna, C.; Ragavendra, C. C.; Beekam, C. S.; Boluvar, L. S.; Nagaral, M. and Rangappa, S. (2021). Synthesis and mechanical characterization of Si3N4 reinforced copper-tin matrix composites. Journal of the Mechanical Behavior of Materials, 30(1), 199-206.

Hayat, M. D.; Singh, H.; He, Z. and Cao, P. (2019). Titanium Metal Matrix Composites: An Overview. Composites Part A: Applied Science and Manufacturing, 121:418-438.

Heimann, R.B. (2023). Silicon Nitride Ceramics: Structure, Synthesis, Properties, and Biomedical Applications. Materials 2023, 16, 5142.

Huang, L. and Geng, L. (2017). Discontinuously reinforced titanium matrix composites. Berlin, Germany: Springer, 1-15.

Hussain, Z.; Jang, H.; Choi, H. and Choi, B. S. (2022). Microstructure, mechanical behavior, and thermal conductivity of three-dimensionally interconnected hexagonal boron nitride-reinforced Cu-Ni composite. Journal of Materials Engineering and Performance, 1-9.

Inagaki, I.; Takechi, T.; Shirai, Y. and Ariyasu, N. (2014). Application and features of titanium for the aerospace industry. Nippon Steel & Sumitomo Metal Technical Report, 106(106), 22-27.

Jawaid, M. and Thariq, M. (2018). Sustainable Composites for Aerospace Applications. Woodhead Publishers, Duxford, United Kingdom.

Jeje, S. O.; Shongwe, M. B.; Maledi, N.; Rominiyi, A. L.; Adesina, O. S. and Olubambi, P. A. (2021b).

Synthesis and characterization of TiN nanoceramic reinforced Ti–7Al–1Mo composite produced by spark plasma sintering. Materials Science and Engineering: A, 807, 140904.

Jeje, S. O., Shongwe, M. B., Rominiyi, A. L. and Olubambi, P. A. (2021a). Spark plasma sintering of titanium matrix composite—a review. The International Journal of Advanced Manufacturing Technology, 117(9), 2529-2544.

Jiang, X.; Weng, Q.; Wang, X.; Li, X.; Zhang, J.; Golberg, D. and Bando, Y. (2015). Recent Progress on Fabrications and Applications of Boron Nitride Nanomaterials: A Review. Journal of Materials Science & Technology, 31(6):589-598.

Kaliappan, S.; Shanmugam, A.; Johnson, P.; Karthick, M.; Sekar, S.; Patil, P. P.; Sai, M. K. S.; Yuvaraj, K. P. and Govindaraajan, V. (2022). Impact of AlN-SiC Nanoparticle Reinforcement on the Mechanical Behavior of Al 6061-Based Hybrid Composite Developed by the Stir Casting Route. Advances in Materials Science and Engineering, 2022.

Karabacak, A. H.; Çanakçı, A.; Celebi, M.; Güler, O.; Tunc, S. A. and Arpacı, K. A. (2023). Production of Al2024/h-BN nanocomposites with improved corrosion, wear and mechanical properties. Materials Chemistry and Physics, 300, 127566.

Kessel, H. U.; Hennicke, J.; Kirchner, R. and Kessel, T. (2009). Rapid Sintering of Novel Materials by FAST/SPS – Further Development to the Point of an Industrial Production Process with High-Cost Efficiency. FCT Systeme GmbH, 1-11.

Kganakga, M. G.; Prieto, G.; Falodun, O. E.; Tuckart, W. R.; Obadele, B. A.; Ajibola, O. O. and Olubambi, P. A. (2020). Erosion wear behavior of spark plasma-sintered Ti-6Al-4V reinforced with TiN nanoparticles. The International Journal of Advanced Manufacturing Technology, 110, 3051-3060.

Kgoete, F. M., Popoola, A. P. I.; Fayomi, O. S. I. and Adebiyi, I. D. (2018a). Influence of Si_3N_4 on Ti-6Al-4V via spark plasma sintering: Microstructure, corrosion and thermal stability. Journal of Alloys and Compounds, 763, 322-328.

Kgoete, F. M.; Popoola, A. P. and Fayomi, O. S. (2019). Oxidation Resistance of Spark Plasma Sintered Ti6Al4V-TiN Composites. Journal of Alloys and Compounds, 772:943-948.

Kgoete, F. M.; Popoola, A. P. I. and Fayomi, O. S. I. (2018b). Influence of spark plasma sintering on microstructure and corrosion behaviour of Ti-6Al-4V alloy reinforced with micron-sized Si_3N_4 powder. Defence Technology, 14(5), 403-407.

Kgoete, F. M.; Popoola, A. P. I.; Fayomi, O. S. I. and Adebiyi, I. D. (2018c). Spark plasma sintered Ti6Al4V-Si_3N_4-TiN ternary composites: Effect of combined microsized Si_3N_4 and TiN addition on microstructure and mechanical properties for aerospace application. Journal of Alloys and Compounds, 769, 817-823.

Khalaj, M.; Zarabi, G. S.; Alem, S. A. A.; Baghchesaraee, K.; Hasanzadeh, A. M. and Angizi, S. (2020). Recent progress in the study of thermal properties and tribological behaviors of hexagonal boron nitride-reinforced composites. Journal of Composites Science, 4(3), 116.

Khrustalyov, A. P.; Vorozhtsov, S. A.; Zhukov, I. A.; Promakhov, V. V.; Dammer, V. K. and Vorozhtsov, A. B. (2017). Structure and mechanical properties of magnesium-based composites reinforced with nitride aluminum nanoparticles. Russian Physics Journal, 59, 2183-2185.

Kim, I. Y.; Choi, B. J.; Kim, Y. J. and Lee, Y. Z. (2011). Friction and Wear Behavior of Titanium Matrix (TiB+ TiC) Composites. Wear, 271:1962-1965

Kim, K. K.; Hsu, A.; Jia, X.; Kim, X. M.; Shi, Y.; Hofmann, M.; Nezich, D.; Rodriguez-Nieva, J. F.; Dresselhaus, M.; Palacios, T. and Kong, J. (2012). Synthesis of Monolayer Hexagonal Boron Nitride on Cu Foil Using Chemical Vapor Deposition. Nano Letter, 12, 161-166.

Klemm, H. (2010). Silicon nitride for high-temperature applications. Journal of the American Ceramic Society, 93(6), 1501-1522.

Klöpfer, C. (2006). Boron nitride–solutions for aluminum extrusion. Aluminium-Dusseldorf Then Isernhagen-Aluminium Verlag GMBH, 82(5), 389-395.

Kondoh, K. (2015). Titanium Metal Matrix Composites by Powder Metallurgy (PM) Routes. Butterworth-Heinemann Publisher, Boston.

Krishna, B.; Balaji, M. and Prakash, P.C. (2022). Experimental investigation of magnesium matrix composite reinforced with titanium nitride nanoparticles. International Research Journal of Engineering and Technology (IRJET), 9(10), 352-357.

Kumar, A.; Rana, R. S.; Purohit, R.; Saxena, K. K.; Xu, J. and Malik, V. (2022). Metallographic Study and Sliding Wear Optimization of Nano Si_3N_4 Reinforced High-Strength Al Metal Matrix Composites. Lubricants, 10(9), 202.

Kumar, G. V.; Panigrahy, P. P.; Nithika, S.; Pramod, R. and Rao, C. S. P. (2019). Assessment of mechanical and tribological characteristics of Silicon Nitride reinforced aluminum metal matrix composites. Composites Part B: Engineering, 175, 107138.

Kumar, V. M. and Venkatesh, C. V. (2019). Evaluation of microstructure, physical and mechanical properties of Al 7079–AlN metal matrix composites. Materials Research Express, 6(12), 126503.

Lad, R. J. (1996). Surface Structure of Crystalline Ceramics. Handbook of Surface Science, 1, 185-228.

Lagos, M. A.; Agote, I.; Atxaga, G.; Adarraga, O. and Pambaguian, L. (2016). Fabrication and Characterization of Titanium Matrix Composites Obtained Using a Combination of Self-Propagating High Temperature Synthesis and Spark Plasma Sintering. Materials Science and Engineering: A, 655, 44-49.

Leyens, C. and Peters, M. (2003). Titanium and Titanium Alloys: Fundamentals and Applications. John Wiley & Sons Publisher, New Jersey, USA.

Li, C.; Lv, X.; Wu, X.; Chen, J.; Liu, X. and Pang, L. (2019). Nano-sized TiN-reinforced composites: Fabrication, microstructure, and mechanical properties. Journal of Materials Research, 34(15), 2582-2589.

Lipp, A.; Schwetz, K. A. and Hunold, K. (1989). Hexagonal boron nitride: Fabrication, properties and applications. Journal of the European Ceramic Society, 5(1), 3-9.

Liu, D.; Zhang, S. Q.; Li, A. and Wang, H. M. (2009). Microstructure and tensile properties of laser melting deposited TiC/TA15 titanium matrix composites. Journal of alloys and compounds, 485(1-2), 156-162.

Liu, S.; Long, M.; Zhang, S.; Zhao, Y.; Zhao, J.; Feng, Y.; Chen, D. and Ma, M. (2020). Study on the Prediction of Tensile Strength and Phase Transition for Ultra-High Strength Hot Stamping Steel. Journal of Materials Research and Technology, 9(6):14244-14253.

Liu, Y.; Chen, L. F.; Tang, H. P.; Liu, C. T.; Liu, B. and Huang, B. Y. (2006). Design of powder metallurgy titanium alloys and composites. Materials Science and Engineering: A, 418(1-2), 25-35.

Liu, Y. Q.; Cong, H. T.; Wang, W.; Sun, C. H. and Cheng, H. M. (2009). AlN nanoparticle-reinforced nanocrystalline Al matrix composites: Fabrication and mechanical properties. Materials Science and Engineering: A, 505(1-2), 151-156.

López-López, I. I.; Contreras, A.; Morales-Estrella, R. and Lemus-Ruiz, J. (2023). Kinetics evaluation of passive oxidation at high temperature of silicon nitride used in the fabrication of lightweight metal matrix composites. Silicon, 15(7), 3181-3192.

Lopez-Suarez, A.; Rickards, J. and Trejo-Luna, R. (2003). Analysis of hydrogen absorption by Ti and Ti–6Al–4V using the ERDA technique. International journal of hydrogen energy, 28(10), 1107-1113.

Lu, J. F.; Zhang, Z. H.; Liu, Z. F. and Wang, F. C. (2015). Sintering mechanism of Ti-6Al-4V prepared by SPS. Applied Mechanics and Materials, 782, 97-101.

Lütjering, G. and Williams, J. C. (2007). Titanium Matrix Composites. Springer Berlin Heidelberg, Germany, 367-382.

Ma, X.; Zhao, Y. F.; Tian, W. J.; Qian, Z.; Chen, H. W.; Wu, Y. Y. and Liu, X. F. (2016). A novel Al matrix composite reinforced by nano-AlNp network. Scientific Reports, 6(1), 34919.

Maddaiah, K. C. and Veeresh Kumar, G. B. (2023). Mechanical Characterization of AA357 Metal Matrix Composite with Reinforcement of Si3N4. Journal of Testing and Evaluation, 51(5), 3255-3272.

Mahato, A. and Mondal, S. (2021). Fabrication and microstructure of micro and nano silicon carbide reinforced copper metal matrix composites/nanocomposites. Silicon, 13(4), 1097-1105.

Mahesh, L.; Reddy, J. S.; Jagadeesh, L. R. and Vinyas, M. (2020). The study of microstructure and wear behaviour of titanium nitride reinforced aluminium. Presented at the 2nd International Conference on Emerging Research in Civil, Aeronautical and Mechanical Engineering (ERCAM 2019), Bangalore, India.

Maja, M. E.; Falodun, O. E.; Obadele, B. A.; Oke, S. R. and Olubambi, P. A. (2018). Nanoindentation studies on TiN nanoceramic reinforced Ti–6Al–4V matrix composite. Ceramics International, 44(4), 4419-4425.

Manghnani, S.; Shekhawat, D.; Goswami, C.; Patnaik, T. K. and Singh, T. (2021). Mechanical and tribological characteristics of Si_3N_4 reinforced aluminium matrix composites: A short review. Materials Today: Proceedings, 44, 4059-4064.

Maseko, S. W.; Popoola, A. P. I. and Fayomi, O. S. I. (2018). Characterization of Ceramic Reinforced Titanium Matrix Composites Fabricated by Spark Plasma Sintering for Anti-Ballistic Applications. Defence Technology, 14(5):408-411.

Matizamhuka, W. R. (2016). Spark Plasma Sintering (SPS) – An Advanced Sintering Technique for Structural Nanocomposite Materials. The Journal of the South African Institute of Mining and Metallurgy, 16:1171-1180.

Mattli, M. R.; Matli, P. R.; Shakoor, A. and Amer, M. A. M. (2019). Structural and mechanical properties of amorphous Si3N4 nanoparticles reinforced Al matrix composites prepared by microwave sintering. Ceramics, 2(1), 126-134.

Milošev, I.; Strehblow, H. H. and Navinšek, B. (1997). Comparison of TiN, ZrN and CrN hard nitride coatings: Electrochemical and thermal oxidation. Thin solid films, 303(1-2), 246-254.

Moghadam, A. D.; Schultz, B. F.; Ferguson, J. B.; Omrani, E.; Rohatgi, P. K. and Gupta, N. (2014). Functional Metal Matrix Composites: Self-Lubricating, Self-Healing, and Nanocomposites - An Outlook. The Journal of the Minerals, Metals and Materials Society, 66:872-881.

Morkoç, H. (2001). Aluminum, gallium, and indium nitrides. Encyclopedia of Materials: Science and Technology, 121-126.

Mouritz, A. P. (2012). Introduction to Aerospace Materials. Woodhead Publisher, Cambridge, United Kingdom.

Mutuk, T. and Gürbüz, M. (2021). Mechanical and wear properties of Si_3N_4 reinforced titanium composites. Indian Journal of Engineering and Materials Sciences (IJEMS), 27(5), 1027-1036.

Niinomi, M.; Liu, Y., Nakai, M.; Liu, H. and Li, H. (2016). Biomedical titanium alloys with Young's moduli close to that of cortical bone. Regenerative Biomaterials, 3(3), 173-185.

Nsiah-Baafi, E.; Andrews, A.; Diouf, S. and Olubambi, P. A. (2022). Wear and Corrosion Properties of Spark Plasma Sintered Ti6Al4V–Al2O3 Composites. Open Ceramics, 10:100260.

Ogunmefun, O. A.; Olubambi, P. A.; Bayode, B. L.; Anamu, U.; Olorundaisi, E.; Ayodele, O.; Babalola, B.; Mkhatshwa, S.; Odetola, P. and Ngeleshi, K. (2024). Densification, microstructure, and nanomechanical evaluation of pulsed electric sintered zirconia-silicon nitride reinforced Ti-6Al-4 V alloy. The International Journal of Advanced Manufacturing Technology, 130(7), 3649-3660.

Okoro, A. M.; Machaka, R.; Lephuthing, S. S.; Oke, S. R.; Awotunde, M. A. and Olubambi, P. A. (2019). Evaluation of the Sinterability, Densification Behaviour and Microhardness of Spark Plasma Sintered Multiwall Carbon Nanotubes Reinforced Ti6Al4V Nanocomposites. Ceramics International, 45(16):19864-19878.

Panda, K. B. and Ravi C. K.S. (2003). Synthesis of ductile titanium-titanium boride (Ti-TiB) composites with a beta-titanium matrix: The nature of TiB formation and

composite properties. Metallurgical and materials transactions A, 34, 1371-1385.

Parveen, A.; Chauhan, N. R. and Suhaib, M. (2019). Study of Si3N4 reinforcement on the morphological and tribomechanical behaviour of aluminium matrix composites. Materials Research Express, 6(4), 042001.

Paulraj, P. and Harichandran, R. (2020). The tribological behavior of hybrid aluminum alloy nanocomposites at High temperature: Role of nanoparticles. Journal of Materials Research and Technology, 9(5), 11517-11530.

Pierson, H. O. (1996). Handbook of Refractory Carbides and Nitrides: Properties, Characteristics, Processing and Applications. Noyes Publisher, Park Ridge, Norwich.

Pradhan, S.; Jena, S. K.; Patnaik, S. C.; Swain, P. K. and Majhi, J. (2015). Wear characteristics of Al-AlN composites produced in-situ by nitrogenation. Presented at the 4th National Conference on Processing and Characterzation of Materials (CPCM 2014), Rourkela, India.

Qian, M.; Yang, Y. F.; Luo, S. D. and Tang, H. P. (2015). Pressureless sintering of titanium and titanium alloys: sintering densification and solute homogenization. Butterworth-Heinemann Publisher, *Oxford, United Kingdom.*

Radhika, N. and Raghu, R. (2017). Investigation on mechanical properties and analysis of dry sliding Wear behavior of Al LM13/AlN metal matrix composite based on Taguchi's technique. Journal of Tribology, 139(4), 041602.

Raja, R.; Jannet, S.; Aby, J. and Dhas, D. E. J. (2022). Study of the mechanical, wear and corrosion behaviour of silicon nitride nanoparticles reinforced copper surface composite through friction stir processing. Engineering Research Express, 4(3), 035025.

Ramaswamy, R.; Marimuthu, P. and Selvam, B. (2016). An Overview on Mechanical Properties of Particulate Reinforced Ti6Al4V Metal Matrix Composites. ARPN Journal of Engineering and Applied Sciences, 11(9):6066-6069.

Ras, M. A.; May, D.; Winkler, T.; Michel, B.; Rzepka, S. and Wunderle, B. (2014). Thermal characterization of highly conductive die attach materials. Presented at the 20th International Workshop on Thermal Investigations of ICs and Systems (THERMINIC 2014), Greewich, London, 1-7, UK: IEEE.

Reddy, A. C. (2003). Thermal Expansion Studies on Aluminum Matrix Composites with Different Reinforcement Volume Fractions of Si_3N_4 Nanoparticles. Presented at the 4th International Conference on Composite Materials and Characterization (ICCMC 2003), Hyderabad, India, 221-225.

Reddy, A. C. (2013). Thermal Expansion of Al Matrix Composites Reinforced with TiN Nanoparticles. Presented at the 2nd International Conference on Thermal and Tribological Behavior of Composites (ICTTBC 2013), New Delhi, India, 144-148.

Reddy, M. P.; Manakari, V.; Parande, G.; Ubaid, F.; Shakoor, R. A.; Mohamed, A. M. A. and Gupta, M. (2018). Enhancing compressive, tensile, thermal and damping response of pure Al using BN nanoparticles. Journal of Alloys and Compounds, 762, 398-408.

Riedel, R. (2000). Handbook of Ceramic Hard Materials. WILEY-VCH Verlag GmbH Publisher, Weinheiin, Federal Republic of Germany.

Riley, F. L. (2000). Silicon nitride and related materials. Journal of the American Ceramic Society, 83(2), 245-265.

Rohatgi, P. K.; Tabandeh-Khorshid, M.; Omrani, E.; Lovell, M. R. and Menezes, P. L. (2013). Tribology of Metal Matrix Composites. Tribology for Scientists and Engineers: From Basics to Advanced Concepts, 233-268.

Rominiyi, A. L.; Shongwe, M. B.; Tshabalala, L. C.; Ogunmuyiwa, E. N.; Jeje, S. O.; Babalola, B. J. and Olubambi, P. A. (2020). Spark Plasma Sintering of Ti–Ni–TiCN Composites: Microstructural Characterization, Densification and Mechanical Properties. Journal of Alloys and Compounds, 848:156559.

Saheb, N.; Iqbal, Z.; Khalil, A.; Hakeem, A. S.; Al Aqeeli, N.; Laoui, T.; Al-Qutub, A. and Kirchner, R. (2012). Spark Plasma Sintering of Metals and Metal Matrix Nanocomposites: A Review. Journal of Nanomaterials, 18:18.

Salihu, S. A.; Suleiman, Y. I. and Eyinavi, A. I. (2019). Classification, Properties and Applications of Titanium and its Alloys Used in Automotive Industry - A Review. American Journal of Engineering Research, 8(8):92-98.

Saresh, N.; Pillai, M. G. and Mathew, J. (2007). Investigation into the Effect of Electron Beam Welding on Thick Ti6Al4V Titanium Alloy. Journal of Materials Processing Technology, 192:83-88.

Saurabh, A.; Meghana, C. M.; Singh, P. K. and Verma, P. C. (2022). Titanium-based materials: synthesis, properties, and applications. Materials Today: Proceedings, 56, 412-419.

Sharma, P.; Sharma, S. & Khanduja, D. (2015). A Study on Microstructure of Aluminium Matrix Composites. Journal of Asian Ceramic Societies, 3(3):240-244.

Shen, Z.; Johnsson, M. and Nygren, M. (2003). TiN/Al_2O_3 composites and graded laminates thereof consolidated by spark plasma sintering. Journal of the European Ceramic Society, 23(7), 1061-1068.

Singerman, S. A.; Jackson, J. J. and Lynn, M. (1996). Titanium metal matrix composites for aerospace applications. Superalloys, 3, 579-586.

Singh, A. K.; Yadav, G. and Gupta, P. (2023). Correlation of Structural and Mechanical Properties for Ultrasonically Stir Casted Al6061 Reinforced SiC-AlN Hybrid Metal Matrix Composites. ECS Journal of Solid-State Science and Technology, 12(5), 057008.

Singh, D. K.; Roul, B. K.; Nanda, K. K. and Krupanidhi, S. B. (2021b). Group III-Nitrides and Their Hybrid Structures for Next-Generation Photodetectors. Light-Emitting Diodes and Photodetectors-Advances and Future Directions.

Singh, J.; Alba-Baena, N.; Trehan, R. and Sharma, V. S. (2022b). Microstructure, Mechanical Properties and Tribological Behavior of A380/Nano-Hexagonal Boron Nitride Metal Matrix Composite. Journal of Materials Engineering and Performance, 31(6), 4887-4901.

Singh, N.; Ummethala, R.; Karamched, P. S.; Sokkalingam, R.; Gopal, V.; Manivasagam, G.; and Prashanth, K. G. (2021a). Spark plasma sintering of Ti6Al4V metal matrix composites: Microstructure, mechanical and corrosion properties. Journal of Alloys and Compounds, 865, 158875

Singh, N.; Ummethala, R.; Surreddi, K. B.; Jayaraj, J.; Sokkalingam, R., Rajput, M., Chatterjee, K. and Prashanth, K. G. (2022a). Effect of TiB_2 addition on the mechanical and biological response of spark plasma sintered Ti6Al7Nb matrix composites. Journal of Alloys and Compounds, 924, 166502.

Sivakumar, G.: Ananthi, V. and Ramanathan, S. (2017). Production and mechanical properties of nano SiC particle reinforced Ti–6Al–4V matrix composite. Transactions of Nonferrous Metals Society of China, 27(1), 82-90.

Song, R.; Zhang, S.; He, Y.; He, T.; Li, H.; Liu, B.; Zhang, Z. and He, Y. (2022). Silicon nitride nanoparticles reinforced the corrosion resistance of Ni-Cu composite coating in simulated seawater solution. Colloids and Surfaces A: Physicochemical and Engineering Aspects, 649, 129427.

Song, Y.; Liu, W.; Sun, Y.; Guan, S. and Chen, Y. (2021). Microstructural evolution and mechanical properties of graphene oxide-reinforced Ti6Al4V matrix composite fabricated using spark plasma sintering. Nanomaterials, 11(6), 1440.

Spengler, W.; Kaiser, R.; Christensen, A. N. and Müller-Vogt, G. (1978). Raman scattering, superconductivity, and phonon density of states of stoichiometric and nonstoichiometric TiN. Physical Review B, 17(3), 1095.

Stone, D. S.; Yoder, K. B. and Sproul, W. D. (1991). Hardness and elastic modulus of TiN based on continuous indentation technique and new correlation. Journal of Vacuum Science & Technology A: Vacuum, Surfaces, and Films, 9(4), 2543-2547.

Tanwir, M. T. A.; Azhar, M. A. and Yasser, Y. R. (2023). Physical, mechanical and morphological characterization of A356/Si_3N_4 nanoparticles stir casting composites. Journal of Engineering Research, 11(3).

Toth, L. (2014). Transition metal carbides and nitrides. Academic Press Elsevier Publisher, Cambridge, Massachusetts, USA.

Tsang, H. T.; Chao, C. G. and Ma, C. Y. (1997). Effects of volume fraction of reinforcement on tensile and creep properties of in-situ TiB/Ti MMC. Scripta Materialia, 37(9), 1359-1365.

Ujah, C. O.; Popoola, A. P.; Popoola, O. M. and Aigbodion, V. S. (2018). Optimization of Spark Plasma Sintering Parameters of Al-CNTs-Nb Nano-Composite Using Taguchi Design of Experiment. The International Journal of Advanced Manufacturing Technology, 100(5):1563-1573.

Van Tran, C. and La, D. D. (2018). Synthesis of silicon nitride ceramic material using direct nitridation process. International Journal of Advanced Engineering Research and Science, 5(8), 264229.

Vasanthakumar, K.; Ghosh, S.; Koundinya, N. T. B. N.; Ramaprabhu, S. and Bakshi, S. R. (2019). Synthesis and mechanical properties of TiCx and Ti (C, N) reinforced Titanium matrix in situ composites by reactive spark plasma sintering. Materials Science and Engineering: A, 759, 30-39.

Veiga, C.; Davim, J. P. and Loureiro, A. J. R. (2012). Properties and applications of titanium alloys: a brief review. Reviews on Advanced Materials Science, 32(2), 133-148.

Wang, F. C.; Zhang, Z. H.; Sun, Y. J.; Liu, Y.; Hu, Z. Y.; Wang, H.; Korznikov, A. V.; Korznikova, E.; Liu, Z. F. and Osamu, S. (2015). Rapid and low temperature spark plasma sintering synthesis of novel carbon nanotube reinforced titanium matrix composites. Carbon, 95, 396-407.

Wang, X.; Liu, K.; Su, Y.; Wang, X.; Cao, H.; Hua, A.; Ouyang, Q. and Zhang, D. (2022). Synergistic enhancing effect of tungsten-copper coated graphite flakes and aluminum nitride nanoparticles on microstructure, mechanical and thermal properties of copper matrix composites. Materials Science and Engineering: A, 857, 143987.

Ward, C. H.; Williams, J. C.; Thompson, A. W.; Rosenthal, D. G. and Froes, F. H. (1989). Fracture mechanisms in titanium aluminide intermetallics. Memoires Scientifiques de La Revue de Metallurgie, 86(10), 647-653.

Wei, S.; Zhang, Z. H.; Wang, F. C.; Shen, X. B.; Cai, H. N.; Lee, S. K. and Wang, L. (2013). Effect of Ti content and sintering temperature on the microstructures and mechanical properties of TiB reinforced titanium composites synthesized by SPS process. Materials Science and Engineering: A, 560, 249-255.

Williams, J. C. and Boyer, R. R. (2020). Opportunities and Issues in the Application of Titanium Alloys for Aerospace Components. Metals, 10(705):1-22.

Xiang, W.; Xuliang, M.; Xinlin, L.; Lihua, D. and Mingjia, W. (2012). Effect of Boron Addition on Microstructure and Mechanical Properties of TiC/Ti6Al4V Composites. Materials & Design, 36:41-46.

Yamanoglu, R.; Daoud, I. and Olevsky, E. A. (2018). Spark plasma sintering versus hot pressing–densification, bending strength, microstructure, and tribological properties of Ti5Al2. 5Fe alloys. Powder Metallurgy, 61(2), 178-186.

Yan, Z.; Chen, F.; Cai, Y. and Zheng, Y. (2014). Microstructure and mechanical properties of in-situ synthesized TiB whiskers reinforced titanium matrix composites by high-velocity compaction. Powder Technology, 267, 309-314.

Zhang, B.; Zhang, F.; Saba, F. and Shang, C. (2021). Graphene-TiC hybrid reinforced titanium matrix composites with 3D network architecture: Fabrication, microstructure and mechanical properties. Journal of Alloys and Compounds, 859, 157777.

Zhang, F.; Reich, M.; Kessler, O. and Burkel, E. (2013). The Potential of Rapid Cooling Spark Plasma Sintering for Metallic Materials. Materials Today, 16 (5):193-197.

Zhang, R. Q.; Lee, T. H.; Yu, B. D.; Stampfl, C. and Soon, A. (2012). The role of titanium nitride supports for single-atom platinum-based catalysts in fuel cell technology. Physical Chemistry Chemical Physics, 14(48), 16552-16557.

Zheng, Z.; Cox, M. and Li, B. (2018). Surface modification of hexagonal boron nitride nanomaterials: a review. Journal of Materials Science, 53, 66-99.

Zhu, X.; Wei, X.; Huang, Y.; Wang, F. and Yan, P. (2019). High-temperature friction and wear properties of NiCr/hBN self-lubricating composites. Metals, 9(3), 356.